DOKUZ EYLÜL UNIVERSITY
GRADUATE SCHOOL OF NATURAL AND APPLIED SCIENCES

A NUMERICAL STUDY ON THE THERMAL EXPANSION COEFFICIENTS OF FIBER REINFORCED COMPOSITE MATERIALS

by

Ziya Haktan KARADENİZ

July, 2005

İZMİR

A NUMERICAL STUDY ON THE THERMAL EXPANSION COEFFICIENTS OF FIBER REINFORCED COMPOSITE MATERIALS

A Thesis Submitted to the
Graduate School of Natural and Applied Sciences of Dokuz Eylül University
In Partial Fulfillment of the Requirements for the Degree of
Master of Science in Mechanical Engineering, Energy Program

by
Ziya Haktan KARADENİZ

July, 2005
İZMİR

M.Sc THESIS EXAMINATION RESULT FORM

We have read the thesis entitled **"A NUMERICAL STUDY ON THE THERMAL EXPANSION COEFFICIENTS OF FIBER REINFORCED COMPOSITE MATERIALS"** completed by **Ziya Haktan KARADENİZ** under supervision of **Assist. Prof. Dr. Dilek KUMLUTAŞ** and we certify that in our opinion it is fully adequate, in scope and in quality, as a thesis for the degree of Master of Science.

.....

Assist. Prof. Dr. Dilek KUMLUTAŞ

Supervisor

.....

(Jury Member)

.....

(Jury Member)

Prof.Dr. Cahit HELVACI
Director
Graduate School of Natural and Applied Sciences

ACKNOWLEDGEMENTS

I would like to thank to my supervisor Assist. Prof. Dr. Dilek KUMLUTAŞ for her guidance, valuable advises, incomparable helps and considerable concern in carrying out the study.

I would especially like to thank to my family for their helpful encouragement and valuable support.

Finally, I would like to thank my fiancée for her unconditional friendship, unlimited patience, moral support and unconditional love.

A NUMERICAL STUDY ON THE THERMAL EXPANSION COEFFICIENTS OF FIBER REINFORCED COMPOSITE MATERIALS

ABSTRACT

In the present work, the effective CTE of different kinds of fiber reinforced composites is studied by micromechanical modeling using finite element method. To determine the both longitudinal and transverse CTEs of composites, three dimensional steady state analyses were undertaken. Representative unit cell models, cylinder which is embedded in a cube with unit dimension, having different fiber volume fractions were produced using finite element program ANSYS. Fibers are assumed to have a square packing arrangement. To compare the results of finite element solutions for different types of composites with the results of the analytical methods and to determine the expansion behavior of different material systems with respect to fiber content, models having fiber volume fractions from 10% to 80% with increments of 10% have been composed. Furthermore, comparison between finite element solutions and experimental results have been made upon the models having 40%, 47%, 48%, 54%, 57%, 63%, 65%, and 68% fiber volume fractions.

Present numerical finite element solution by ANSYS is in excellent agreement with the analytical solution by Rosen and Hashin and in sufficient agreement with other analytical solutions. The comparisons of these model predictions with experimental data show that for some material the agreement is very good, but for others there is some discrepancy between the experimental results and model predictions. The reason may be that the fiber-matrix interface bond which was assumed to be perfect was not really so in the experimental materials. The interface may either contain interfacial cracks or it might have elastic properties different from those of matrix and fiber.

Keywords: Coefficient of thermal expansion, fiber reinforced composites, ANSYS, micromechanical modeling.

LİF KATKILI KOMPOZİT MALZEMELERİN ISIL GENLEŞME KATSAYILARI ÜZERİNE SAYISAL BİR ÇALIŞMA

ÖZ

Bu çalışmada, farklı türde lif ve matris malzemelerden oluşan kompozit malzemelerin ısıl genleşme katsayıları önce mevcut analitik yöntemlerle belirlenmiş, daha sonra kompozit malzemelerin mikro yapıları temsili birim hücreler şeklinde modellenerek sonlu elemanlar yöntemiyle çözüm yapan ANSYS programı kullanılarak analizler yapılmıştır. Malzemelerin enine ve boyuna ısıl enleşme katsayılarını belirleyebilmek için birim kenarlı bir küp içine yerleştirilmiş bir silindir şeklinde üç boyutlu mikro yapı modelleri oluşturulmuştur. Liflerin matris malzeme içinde karesel düzende dağıldığı varsayılmıştır.

Lif doğrultusu, miktarı ve türünün malzemenin ısıl genleşme katsayısı üzerindeki etkilerini incelemek ve analitik yöntemlerle sonlu elemanlar yöntemini karşılaştırmak için tüm kompozit malzemelerin %10'luk aralıklarla %10 - %80 aralığında hacimsel lif oranına sahip modelleri oluşturulmuştur. Bununla birlikte elde edilen sonuçları mevcut deney sonuçlarıyla karşılaştırmak için 40%, 47%, 48%, 54%, 57%, 63%, 65% ve 68% hacimsel oranlarında lif içeren modeller oluşturulmuştur.

Sonlu elemanlar yönteminin Rosen-Hashin yöntemiyle iyi uyum gösterdiği diğer analitik yöntemlerle de uyumlu olduğu görülmüştür. Deney sonuçları ile en iyi uyumu sonlu elemanlar yöntemi göstermiştir. Diğer analitik yöntemler ise bazı malzemeler için iyi sonuçlar verirken bazılarında deney sonuçlarına göre yüksek sapma göstermişlerdir. Kompozit malzemenin ısıl genleşme katsayısını belirlemek için sonlu elemanlar yönteminin güvenilir bir yol olduğu görülmüştür.

Anahtar kelimeler: Isıl genleşme katsayısı, lif katkılı kompozitler, ANSYS, mikro yapı modelleri.

CONTENTS

Page

THESIS EXAMINATION RESULT FORM ii
ACKNOWLEDGEMENTS iii
ABSTRACT iv
ÖZ v
CONTENTS vi

CHAPTER ONE – INTRODUCTION 1
1.1 Introduction 1

CHAPTER TWO – FIBER REINFORCED COMPOSITES 7
2.1 Composites 7
2.2 Fiber Reinforced Composites 8
2.2.1 Matrix Materials 8
2.2.1.1 Polymer Matrix Materials 9
2.2.1.2 Metal Matrix Materials 11
2.2.1.3 Ceramic Matrix Materials 12
2.2.2 Fibers 13
2.2.2.1 Boron Fibers 15
2.2.2.2 Carbon Fibers 16
2.2.2.3 Ceramic Fibers 18
2.2.2.4 Glass Fibers 19
2.2.2.5 Organic Fibers 21
2.2.2.5.1 Cellulose Fibers 22
2.2.2.5.2 Oriented Polyethylene Fibers 23
2.2.2.5.3 Aramid Fibers 24
2.2.2.6 Whiskers 26

CHAPTER THREE – THERMAL EXPANSION BEHAVIOUR OF FIBER REINFORCED COMPOSITES 27
3.1 Coefficient of Thermal Expansion (CTE) 27
3.2 Factors Affecting the Coefficient of Thermal Expansion 28
3.2.1 Fiber Volume 28
3.2.2 Void Volume 29
3.2.3 Lay-up Angle 29
3.2.4 Thermal Cycling 30
3.2.5 Temperature Dependence 30
3.2.6 Moisture Effects 30
3.2.7 Viscoelasticty 31
3.3 Thermal Expansion Measurement Techniques 31
3.3.1 Mechanical Dilatometry 32
3.3.2 Interferometry 34
3.3.3 Strain Gauges 36
3.4 Theoretical Consideration 37
3.4.1 Some of the Existing Theories 38
3.4.1.1 Law of Mixtures 38
3.4.1.2 Equation of Thomas 39
3.4.1.3 Equation of Van Fo Fy 40
3.4.1.4 Equation of Cribb 40
3.4.1.5 Equation of Schapery 41
3.4.1.6 Equation of Chamberlain 42
3.4.1.7 Equation of Rosen and Hashin 43
3.4.1.8 Equation of Schneider 44
3.4.1.9 Equation of Chamis 45
3.4.1.10 Equation of Sideridis 45

CHAPTER FOUR – FINITE ELEMENT METHOD 48
4.1 Historical Perspective 48
4.2 Finite Element Analysis Procedure 49

4.2.1 Geometry Creation 49
4.2.2 Mesh Creation and Element Selection 50
4.2.3 Boundary and Loading Conditions 51
4.2.4 Defining Material Properties 52
4.2.5 Displaying Results 53

CHAPTER FIVE – MICROMECHANICAL ANALYIS BY ANSYS 54
5.1 Model Development 54
5.2 Mesh Creation 56
5.3 Material Properties 57
5.4 Boundary Conditions 59
5.5 Solution 59

CHAPTER SIX – RESULTS AND DISCUSSION 61

REFERENCES 73

CHAPTER ONE
INTRODUCTION

1.1 Introduction

Structural composite materials typically consist of a primary load-carrying (stiff and strong) material phase, such as fibers, held together by a binder of matrix material, often an organic polymer. Matrix is soft and weak, and its direct load bearing is negligible. However, the role of matrix is very important for the structural integrity of composites; matrix protects fibers from hostile environments and localizes the effect of broken fibers. In order to achieve particular elastic properties in preferred directions, continuous fibers are usually employed in structures having essentially two dimensional characteristics. For convenience of construction, the fibers in the form of multifilament tows are laid parallel and impregnated with the matrix resin to form an uncured unidirectional lamina as the basic element of construction. The final complex structure is then produced by stacking the individual lamina in an appropriate sequence and orientation, curing under heat and pressure, to form rigid laminate which possesses the directional characteristics required.

The complexities of composite materials are due to the unknown features such as chemical compatibility, wettability, adsorption characteristics and stress development resulting from differences in thermal and moisture expansion, have so far restricted their complete characterization. Understanding the behavior of composites relative to the properties of fiber and matrix materials is desirable not only for the practical purpose of predicting the properties of composites but also for the fundamental knowledge required in developing new materials.

Linear thermal expansion is the fractional change in length of a body when heated or cooled through a given temperature range and usually it is given as a coefficient per unit temperature interval, either as an average over stated range, or as the tangent to the expansion curve at a given temperature. The longitudinal and transverse

coefficients of thermal expansion of the orthotropic unidirectional lamina must be known for design purposes. These composite properties can be experimentally measured, which can be expensive and time consuming when evaluating many different material systems, or predicted using the thermal and mechanical properties of the constituents. Furthermore, as a result of the increasing computer technology, numerical solutions such as finite element analysis are being used to determine the thermal expansion coefficients of composite materials. Since polymer matrix materials typically exhibit thermal expansion coefficients which are much higher than those of fibers and the fiber may be thermally as well as mechanically anisotropic, complex stress states are induced in the composite due to temperature changes.

The problem of relating effective mechanical properties of fiber reinforced composite materials to constituent properties has received considerable attention. Many analytical models exist for the prediction of the coefficients of thermal expansion for unidirectional composites. In the first half of the 20^{th} century the mathematical complexity of the analysis in the various theories had been ranging from the simple netting analysis to sophisticated statistical methods. The various assumptions underlying these theories were not always explicitly stated. In general they tended to be unrealistic simplifications of the physical state of the materials. These simplifications resulted in theories which do not have satisfactory correlation with experimental data. To obtain better theory-experiment correlation, some of the investigators introduced correction factors. But application of these theories became a matter of the user's familiarity and talent, and resulted in a hopeless case of confusion for the researchers. A critique on theories predicting thermoelastic properties of fiber reinforced composite materials was presented by Chamis and Sendeckyj (1968) where they had introduced basic principles of existing theories and had reviewed individual papers.

A number of articles on thermal expansion of fiber reinforced composites had appeared during 1960s in Russian literature (Shapery, 1968). In an important paper by Levin (1967), effective thermal expansion coefficients for two-phase anisotropic

composites with isotropic phases were derived using an extension of Hill's method (1964). Exact relations were given from which composite thermal expansion coefficients may be determined if constituent properties and effective composite moduli are known. In a series of articles by Van Fo Fy (1965, 1966), exact thermal expansion coefficients for matrices reinforced by doubly periodic array of hollow or solid circular continuous fibers were developed by means of a detailed stress analysis.

Another method for calculating upper and lower bounds on thermal expansion coefficients of isotropic and anisotropic composites with isotropic phases, and some explicit formulas for volumetric and linear coefficients of thermal expansion was given by Shapery (1968). In contrast to work by Levin and Van Fo Fy composites with an arbitrary number of different constituents and arbitrary phase geometry can be treated by Shapery's formula. His method employed the complementary and potential energy principles of thermoelasticity theory in conjunction with a procedure for minimizing the difference between upper and lower bounds. It was shown that for some important cases the bounds coincide and therefore yield exact solutions. Shapery's formula has been the most useful solution to determine the longitudinal thermal expansion coefficient afterwards.

An alternative model for transverse thermal expansion of unidirectional composites was derived by Chamberlain (Rogers et al., 1977), using plane stress thick walled cylinder equations for the case of transversely isotropic fibers embedded in an isotropic cylindrical matrix.

Rosen and Hashin (1970) developed relations to determine the upper and lower bounds on effective thermal expansion coefficients of anisotropic composites having any number of anisotropic phases using thermoelastic energy principles. The bounds they found are complicated algebraic expressions but reduction to simpler form is possible when symmetry of the phases and composite is taken into account. For isotropic phases, the thermal expansion results reduce to the bounds obtained by Shapery (1968). When the composite has only two phases, thermal expansion

coefficients coincide to give results in the form of unique functions of the elastic moduli.

Another consideration was made by Sideridis (1994) who developed the model of the inhomogeneous boundary interphase. He studied the influence of the mode of variation of boundary's thermal expansion coefficient, elastic modulus and Poisson's ratio versus the polar radius between the fiber and the matrix in the representative volume element of a unidirectional fiber composite on the overall value of the composite thermal expansion coefficients. He also made experiments on E-glass-epoxy composites and showed that for all volume fractions the thermal expansion values derived from his solutions are similar to both experiments and the respective values derived from the equations of Shapery and Van Fo Fy.

An analytical and experimental investigation on thermal expansion coefficients of unidirectional composites was carried out by Ishikava, Koyama and Kobayashi (1978). The fiber anisotropy and temperature dependency of the constituent material properties were considered in the formulation of the problem. The solving technique they used was constructed by a slight modification of their previous investigation to calculate elastic moduli of unidirectional composites. The first point of the main purpose of the experiments was to reveal certain temperature dependent behavior of thermal expansion coefficient's of the constituents of carbon-epoxy composites. The second was a comparison between the experimental and theoretical results and the third was to estimate unknown properties of carbon fibers.

The influence of fiber type and orientation on thermal expansion coefficient of carbon-epoxy composites was discussed by Rogers et al. (1977). Interferometric measurements of the linear thermal expansion coefficients between approximately 90-400 K for a series of unidirectional and bidirectional specimens of epoxy resins reinforced with carbon fibers were made. The room temperature results shoved that linear thermal expansion coefficients of these composites are mostly influenced by the thermal and elastic properties of the constituents and the orientation of the fibers. At higher temperatures their results clearly showed significant changes in the

temperature dependence of the dimensional behavior which results from softening of the resin.

The elastic solution achieved by Foye in 1968 employed the finite element method for the first time in the field of micromechanical analysis of unidirectional composites (Adams & Crane, 1984). This generalized plane strain study included two fiber arrangements, separate and combined loading of five of the six components of stress, contours of stresses in the matrix around a fiber, determination of unidirectional lamina composite properties and an evaluation of the accuracy of the various finite element models.

Adams and Crane (1984) modeled a microscopic region of a unidirectional composite by finite element micromechanical analysis using generalized plane strain formulation, but including longitudinal shear loading. Their analysis was capable of treating elastic, transversely isotropic fiber materials, as well as isotropic, elastoplastic materials. They used the micromechanical analysis to predict the stress/strain response into the inelastic range of graphite-epoxy laminate. Their results were in excellent agreement with available experimental data.

Some of analytical models are critically reviewed and compared with experimental measurements by Bowles and Tompkins (1989). For the most part, large discrepancies between the predicted values of the transverse CTE and the test data are observed, except for the model of Rosen and Hashin (1970). Bowles and Tompkins (1989) also conducted finite element calculations for two cell geometries, including doubly periodic square and hexagonal patterns, and showed that their results were in good agreement with the experimental values and with the Rosen-Hashin (1970) analysis. The solution for the periodic square pattern provides the reference for the present investigation.

The thermal expansion response of macroscopically isotropic metal–ceramic composites was studied through micromechanical modeling by Shen (1998). He carried out three-dimensional finite element analyses for the entire range of phase

concentration from pure metal to pure ceramic, using the aluminum–silicon carbide composite as a model system. Particular attention was devoted to the effects of phase connectivity, since other geometrical factors such as the phase shape and particle distribution play a negligible role in affecting the overall coefficient of thermal expansion (CTE) of the composite.

Islam et al. (2001) studied the linear thermal expansion coefficients of unidirectional composites systematically by the finite element method. Thermal expansion coefficients were first determined for composites with perfectly bonded interface between fiber and matrix. Results are compared with available experimental and analytical results. Next cracks caused by debonding along the fiber-matrix interface were studied to investigate the effects of interface cracking on the transverse thermal expansion coefficients.

A combined experimental and numerical methodology for the evaluation of fiber properties from the composite macro-data was presented by Rupnowski et al. (2005). The methodology was based on the measurements of the elastic and thermal macro properties of unidirectional and woven composites by the three-component oscillator resonance method and dilatometry. It is then followed by extraction of the fiber properties using the Eshelby/Mori-Tanaka model for unidirectional and finite element representative unit cells for woven systems.

The aim of this study is to determine the thermal expansion coefficients of composite materials using finite element method. A representative unit cell is used to model the micro-structure of composite materials and the obtained results are compared with available experimental data and analytical methods. It has been seen that finite element method is a good approach to find the thermal expansion coefficients of composite materials.

CHAPTER TWO
FIBER REINFORCED COMPOSITES

2.1 Composites

Composite materials are constructed from two or more elements to produce a material that has different properties from the individual elements. The constituent parts of a composite are the matrix and the reinforcement. The matrix acts as the bulk material and transfers load between reinforcement materials. The matrix also has an additional role, which is to protect the reinforcement from the environment, abrasion and impact. The reinforcement provides the strength and stiffness properties of a composite. The advantage of composite materials is that, if well designed, they usually exhibit the best qualities of their components or constituents and often some qualities that neither constituent possesses. Some of the properties that can be improved by forming a composite material are strength, stiffness, corrosion resistance, wear resistance, attractiveness, weight, fatigue life, temperature dependent behavior, thermal insulation, thermal conductivity, and acoustical insulation (Jones, 1999).

Naturally, neither all of these properties are improved at the same time nor there is usually any requirement to do so. In fact, some of the properties are in conflict with one another such as thermal insulation versus thermal conductivity. The objective is merely to create a material that has only the characteristics needed to perform the design task.

Composite materials have a long history of usage. Their precise beginnings are unknown, but all recorded history contains references to some form of composite material. For example, straw was used by the Israelites to strengthen mud bricks. Plywood was used by the ancient Egyptians when they realized that wood could be rearranged to achieve superior strength and resistance to thermal expansion as well as to swelling caused by the adsorption of moisture. Medieval swords and armor were constructed with layers of different metals. More recently, fiber reinforced, resin matrix composite materials that have

high strength-to-weight and stiffness-to-weight ratios have become important in weight sensitive applications such as aircraft and space vehicles.

Four commonly accepted types of composite materials are:

- Fiber reinforced composite materials that consist of fibers in a matrix.
- Laminated composite materials that consist of layers of various materials.
- Particulate composite materials that are composed of particles in a matrix.
- Combinations of some or all of the first three types.

2.2 Fiber Reinforced Composites

Fiber-reinforced composite materials are increasingly being used in a large variety of structures including aerospace, marine and civil engineering infrastructure fields. Fiber reinforced composite structures offer an attractive alternative to more conventional forms of construction because of their high strength to weight ratio, resistance to corrosion, design flexibility, parts consolidation, electrical insulating properties, dimensional stability and low tooling cost.

The form and arrangement of the fibers vary significantly. They can be arranged as short strands of randomly orientated whiskers, a bundle of fibers, a unidirectional fabric, a woven fabric, a braid (tubular) fabric or a multi-axial fabric. Combinations of reinforcing materials can be utilized to provide a multitude of composite properties, where the material characteristics are aligned with the required performance properties. The selection of the fiber arrangement depends on the loading condition requirements of the component and the constraint on the mass of the resulting component.

2.2.1 Matrix Materials

There are three types of fiber reinforced composites according to matrix materials; polymer matrix composites (PMC), metal matrix composites (MMC) and

ceramic matrix composites (CMC). The most widely used composites are PMCs. These are mainly used in ambient temperature applications. MMCs are commonly used to increase the strength of low density metals. CMCs are used extensively in high temperature applications which require high strength and toughness characteristics. Metal and ceramic matrix composites are relatively new technologies. This is evident when observing the extent of their application, as it is limited to high performance components and assemblies on advanced equipment (Chawla, 1998).

2.2.1.1 Polymer Matrix Materials

Polymers are structurally much more complex than metals or ceramics. They are cheap and can easily be processed. On the other hand, polymers have lower strength and modulus and lower temperature use limits. Prolonged exposure to ultraviolet light and some solvents can cause the degradation of polymer properties. Because of predominantly covalent bonding, polymers are generally poor conductors of heat and electricity. However, they are generally more resistant to chemicals than are metals. Polymers are giant chainlike structures with covalently bonded carbon atoms forming the backbone of the chain. The process of forming large molecules from small ones is called polymerization*;* that is, polymerization is the process of joining many monomers, the basic building blocks, together to form polymers. Different molecular chain configurations of polymers are given in Figure 2.1.

Based on their behavior, there are two major classes of polymers, thermoset and thermoplastic polymers. Polymers that soften or melt on heating are called thermoplastic polymers and are suitable for liquid flow forming. Cooling to room temperature hardens thermoplastics. Their different behavior, however, comes from their molecular structure and shape, molecular size or mass, and the amount and type of bonds (covalent or van der Waals). Examples of thermoplastics include low and high density polyethylene, polystyrene, and polymethyl methacrylate (PMMA).

When the molecules in a polymer are crosslinked in the form of a network, they do not soften on heating. Such cross-linked polymers are called thermosetting

polymers. Thermosetting polymers decompose on heating. Crosslinking makes sliding of molecules past one another difficult, making the polymer strong and rigid. A typical example is that of rubber crosslinked with sulfur which is called vulcanized rubber. Vulcanized rubber has ten times the strength of natural rubber. Common examples of thermosetting polymers include epoxy, phenolic, polyester, vinyl ester, polyurethane, and silicone.

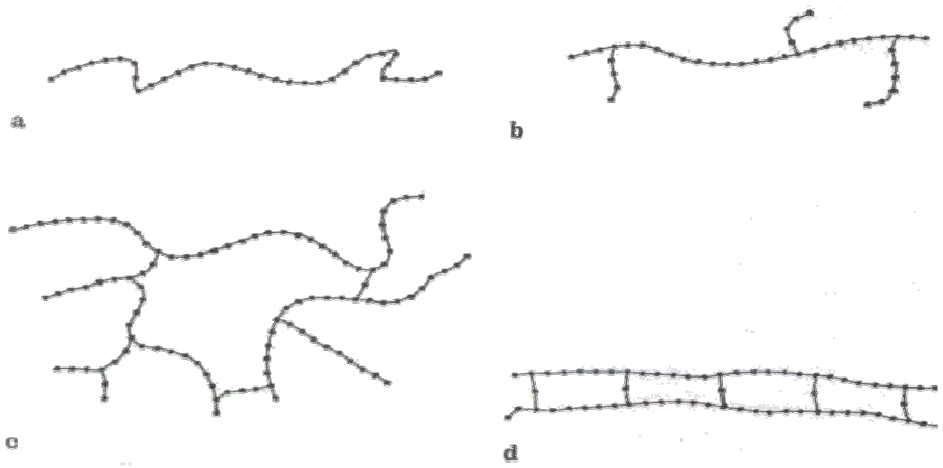


Figure 2.1 Different molecular chain configurations; linear (a), branched (b), crosslinked (c), ladder (d) (Chawla, 1998).

Common types of resin used to provide the composite matrix are polyester, vinyl ester and epoxy. Polymers are not recognized as the strongest of materials, but in the thermosetting resin form they provide excellent abilities to be molded into complex shapes and to adhere strongly to the fibers. Accelerator and catalyst elements can be added to the resins in varying amounts to allow the polymerization reaction to be controlled to provide varying material properties. Use of the catalyst element needs to be carefully controlled to ensure the reaction is not too rapid and to avoid insufficient curing. Polyester resins are the most widely used polymer matrix material; this is maybe due to the fact that they can be used to construct composites without the need to introduce pressure. Vinyl ester resins are similar to polyesters but provide better resistance to chemical and water attack and also display improved toughness. Epoxy resins exhibit higher levels of mechanical strength and they can so be more resilient to environmental attack. The reinforcing materials that are widely used for PMCs are glass, carbon, aramid and boron.

2.2.1.2 Metal Matrix Materials

Metals are extremely versatile engineering materials. A metallic material can exhibit a wide range of readily controllable properties through appropriate selection of alloy composition and thermomechanical processing method. The extensive use of metallic alloys in engineering reflects not only their strength and toughness but also the relative ease and low cost of fabrication of engineering components by a wide range of manufacturing processes. The development of MMCs has reflected the need to achieve property combinations beyond those attainable in monolithic metals alone. Thus, tailored composites resulting from the addition of reinforcements to a metal may provide enhanced specific stiffness coupled with improved fatigue and wear resistance, or perhaps increased specific strength combined with desired thermal characteristics (for example, reduced thermal expansion coefficient and conductivity) in the resulting MMC. However, the cost of achieving property improvements remains a challenge in many potential MMC applications.

MMCs involve distinctly different property combinations and processing procedures as compared to either PMCs or CMCs. This is largely due to the inherent differences among metals, polymers and ceramics as matrix materials and less so to the nature of the reinforcements employed. Pure metals are opaque, lustrous chemical elements and are generally good conductors of heat and electricity. When polished, they tend to reflect light well. Also, most metals are relatively high in density. These characteristics reflect the nature of atom bonding in metals, in which the atoms tend to lose electrons; the resulting free electron "gas" then holds the positive metal ions in place. In contrast, ceramic and polymeric materials are chemical compounds of elements. Bonding in ceramics and intramolecular bonding in polymers is characterized by either sharing of electrons between atoms or the transfer of electrons from one atom to another. The absence of free electrons in ceramics and polymers (no free electrons are formed in polymers due to intermolecular van der Waals bonding) results in poor conductivity of heat and electricity, and lower deformability and toughness in comparison to metallic materials.

Metals are strong and tough. They can be plastically deformed and strengthened by a wide variety of methods. Metal matrix composite construction is used primarily to increase the strength of low density metals such as aluminum alloys, copper, titanium alloys and magnesium alloys. Another reason for constructing MMCs is to increase the wear resistance and higher temperature performance. The matrix material can be reinforced with continuous fibers and wires or by short fibers, whiskers or particles. The complex nature of these materials and their manufacture limits their use to high performance applications, in industries such as, automotive, aerospace, and power. Some of the commonly used reinforcing materials are boron/tungsten, titanium, alumina, graphite and silicon carbide.

Particle or discontinuously reinforced MMCs have become very important because they are less expensive than continuous fiber reinforced composites and they have relatively isotropic properties compared to fiber reinforced composites. Use of nanometer-sized fullerenes (a form of carbon having a large molecule consist of an empty cage of sixty or more carbon atoms, C_{60} is the most common) as a reinforcement has also been tried.

2.2.1.3 Ceramic Matrix Materials

Generally, ceramics consist of one or more metals combined with a nonmetal such as oxygen, carbon or nitrogen. They have strong covalent and ionic bonds. Ceramic materials in general have a very attractive package of properties such as high strength and high stiffness at very high temperatures, chemical inertness, and low density. This attractive package is defaced by one deadly defect; lack of toughness. They are extremely susceptible to thermal shock and are easily damaged during fabrication and/or service. It is therefore understandable that an overriding consideration in ceramic matrix composites is to toughen the ceramics by incorporating fibers in them and thus exploit the attractive high-temperature strength and environmental resistance of ceramic materials without risking a catastrophic failure. There are certain basic differences between CMCs and other composites. The general philosophy in nonceramic matrix composites is to have the fiber bear a greater

proportion of the applied load. This load partitioning depends on the ratio of fiber and matrix elastic moduli, E_f/E_m. In nonceramic matrix composites, this ratio can be very high, while in CMCs, it is rather low and can be as low as unity. Another distinctive point regarding CMCs is that because of limited matrix ductility and generally high fabrication temperature, thermal mismatch between components has a very important bearing on CMC performance. The problem of chemical compatibility between components in CMCs is similar to those in MMCs (Chawla, 1998).

CMCs are highly advanced materials and their use is restricted to applications where high strength or high toughness is required at high temperatures. The high cost of producing CMCs has restricted their use to applications in the power generation and aerospace applications. Silicon carbide and boron nitride and other ceramic fibers are used to reinforce ceramics matrices, such as aluminum oxide and silicon carbide.

2.2.2 Fibers

Fiber is a general term for a filament with a finite length that is at least 100 times its diameter (typically 0.10 to 0.13 mm). They are the most commonly used reinforcing materials in high performance composites as the load bearing component. They must have high thermal stability and should not contract or expand much with temperature. Defects can be placed on the surface to allow the fiber to interact with the matrix, however; bulk defects should be low. In most cases, fibers are prepared by drawing from a molten bath, and spinning or deposition on a substrate. The term fiber is often used synonymously with filament. Some short fibers are called whiskers which are short single-crystal fibers or filaments made from a variety of materials ranging from 1 to 25 microns and aspect ratios between 100 and 15,000. There are many types of fibers used in industrial applications. The most used ones are described below. A comparison of some important characteristics of fiber reinforcement fibers is in Table 2.1.

Table 2.1 Properties of reinforcement fibers (Chawla, 1998).

Property	PAN-Based Carbon		Kevlar[3]49	E-Glass	SiC		Al_2O_3	Boron
	HM[1]	HS[2]			CVD[4]	Nicalon[5]		
Diameter (μm)	7 – 10	7.6 - 8.6	12	8 - 14	100 - 200	10 - 20	20	100 - 200
Density (g/cm^3)	1.95	1.75	1.45	2.55	3.3	2.6	3.95	2.6
Young's modulus (GPa)								
Parallel to fiber axis	390	250	125	70	430	180	379	385
Perpendicular to fiber axis	12	20	–	70	–	–	–	–
Tensile Strength (GPa)	2.2	2.7	2.8 - 3.5	1.5 - 2.5	3.5	2	1.4	3.8
Strain to fracture (%)	0.5	1	2.2 - 2.8	1.8 - 3.2	–	–	–	–
Coefficient of thermal expansion ($10^{-6}/K$)								
Parallel to fiber axis	–0.5 – 0.1	–0.5 - 0.1	–2 - –5	4.7	5.7	–	7.5	8.3
Perpendicular to fiber axis	7 – 12	7 - 12	59	4.7	–	–	–	–

[1] High modulus

[2] Heat stabilized

[3] Trademark of Du Pont

[4] Chemical vapor deposition

[5] Trademark of Nippon Carbon Co.

2.2.2.1 Boron Fibers

Boron is an inherently brittle material. It is commercially made by chemical vapor deposition (CVD) of boron on a substrate, that is, boron fiber is itself a composite as produced (Figure 2.2). Rather high temperatures are required for this deposition process; therefore the choice of substrate material that is used to form the core of the finished boron fiber is limited. A fine tungsten wire or a carbon substrate can be used for this purpose (Chawla, 1998).

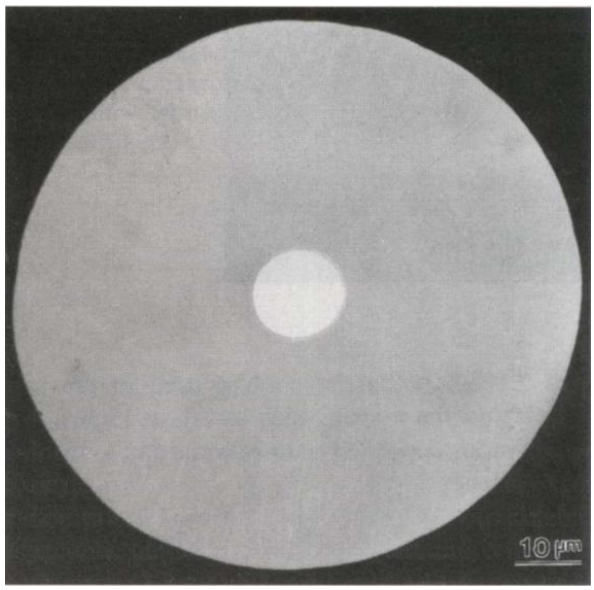
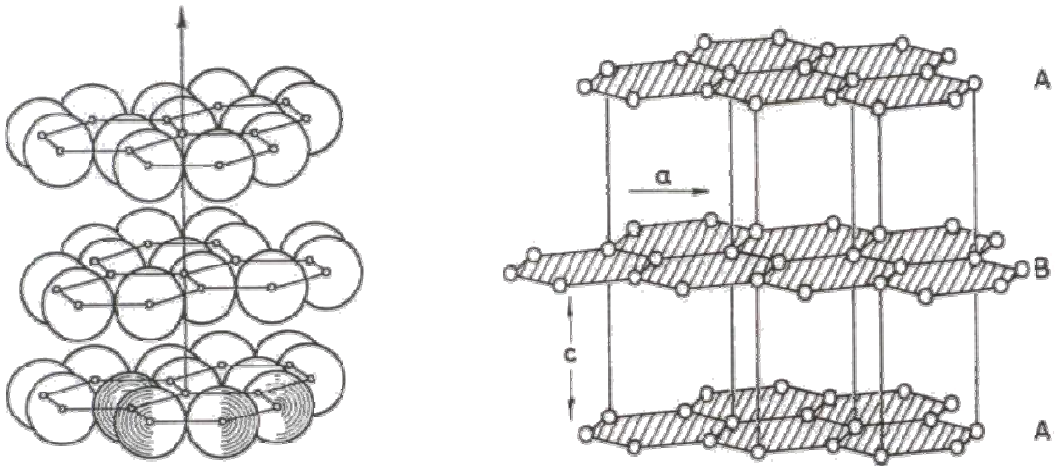


Figure 2.2 Cross section of a 100 μm diameter boron fiber (Chawla, 1998).

The structure and morphology of boron fibers depend on the conditions of deposition; temperature, composition of gasses, gas dynamics, and so on. Complex internal stresses and defects such as voids and structural discontinuities results from the composite nature of boron fibers and decomposition process. Therefore boron fibers don't show the strength of boron. They are used in a number of military aircraft, for stiffening golf shafts, tennis rackets, and bicycle frames. One big obstacle to the widespread use of boron fiber is its high cost compared to other fibers. A major portion of this high price is the cost of the substrate.

2.2.2.2 Carbon Fibers

Carbon is a very light element and can exist in a variety of crystalline forms. Our interest here is in the so-called graphite structure wherein the carbon atoms are arranged in the form of hexagonal layers. Carbon in the graphitic form is highly anisotropic and has a very dense packing (Figure 2.3.a) in the layer planes. The lattice structure is shown more clearly in (Figure 2.3.b). The high-strength bond between carbon atoms in the layer plane results in an extremely high modulus while weak van der Waals type bond between the neighboring layers results in a lower modulus in that direction. Consequently, in a carbon fiber one would like to have a very high degree of preferred orientation of hexagonal planes along fiber direction.

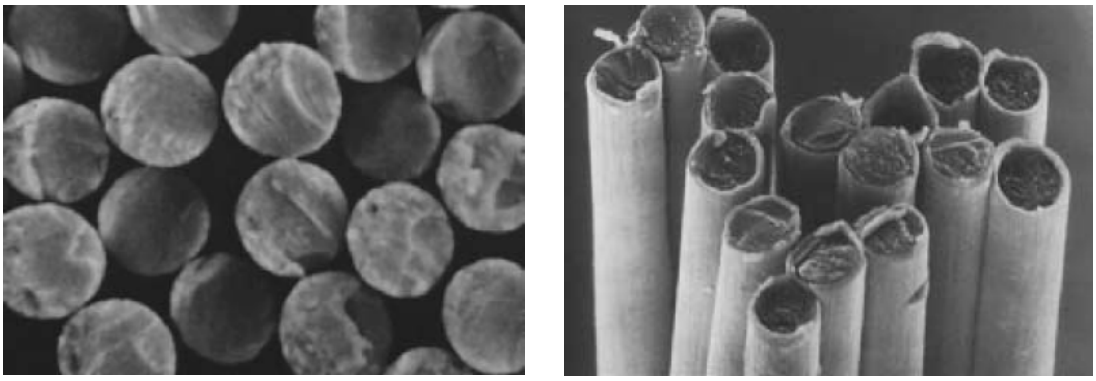


a b

Figure 2.3 The densely packed graphite layer structure (a), and the hexagonal lattice structure of graphite (b) (Chawla, 1998).

Carbon fibers are generally made by carbonization of organic precursor fibers such as polyacrylonitrile (PAN) fibers, rayon and the ones obtained from pitches, polyvinyl alcohol, polyamides, and phenolics. Precursor fibers undergo preoxidation, carbonization and surface treatment. Surface oxidized carbon fibers are also produced to increase adhesion. Also, prepregs are manufactured with various resins (mostly epoxy and bismaleimide) to aid in the incorporation of carbon fibers. The term *prepreg* is a short form of preimpregnated fibers. Prepreg thus represent an intermediate stage in the fabrication of a polymeric composite component. Figure

2.4.a shows micrograph of the cross-section of carbon fiber which can be compared with Figure 2.4.b which shows this fiber coated with nickel. The conditions of carbonization have impact on properties of carbon fibers and their price. The least expensive carbon fibers manufactured from PAN are produced by rapid heating under tension from the initial orientation temperature of 300ºC to 1000ºC. This process produces low modulus fibers. High strength fibers are heated to 1500ºC and the high modulus fibers to 2200ºC under argon. These various conditions result in graphite crystals with different structures which affects the mechanical performance of fibers. Rayon is used less often because of the environmental impact of the precursor material. In the coal-tar or petroleum pitch processes, the initial material is polymerized by heat which helps to remove low molecular weight volatile components. The resultant nematic liquid crystal, or mesophase, is oriented during the spinning operation to form fibers (Wypych, 2000).



a b

Figure 2.4 Micrograph of carbon fibers (a) and nickel coated carbon fibers (b) (Wypych, 2000).

The properties of carbon fibers such as high tensile strength and modulus, good fatigue resistance and wear lubricity, low density (lower than metal), low linear thermal expansion coefficient, good dimensional stability, heat resistance, electrical conductivity, ability to shield electromagnetic waves, x-ray penetrability, good chemical stability and excellent resistance to acids, alkalis, and many solvents are developed their applications. These properties show that carbon fibers have a high potential use in high performance materials. Total world production of carbon fibers is estimated 9,590 tons; North America consumes 40% of total production, Europe and Japan 21% each and the remaining countries 18% (Wypych, 2000). The largest

use is in aircraft industry followed by sport and leisure equipment and industrial equipment.

2.2.2.3 Ceramic Fibers

Although production of ceramic fibers began in the 1940s, their commercial exploitation did not occur until the early 1970s. Worldwide production of ceramic fibers in the early-to-mid 1980s was estimated at 70 to 80 million kg, with U.S. production comprising approximately half that amount. With the introduction of new ceramic fibers for new uses, production has increased significantly over the past decades (IARC, 1988).

Ceramic fibers comprise a wide range of amorphous or crystalline, synthetic mineral fibers characterized by their refractory properties (i.e., stability at high temperatures). They are typically made of alumina, silica, and other metal oxides or, less commonly, of nonoxide materials such as silicon carbide. Most ceramic fibers are composed of alumina and silica in an approximate 50/50 mixture. Monoxide ceramics, such as alumina and zirconia, are composed of at least 80% of one oxide, by definition; generally they contain 90% or more of the base oxide and specialty products may contain virtually 100%. Nonoxide specialty ceramic fibers, such as silicon carbide, silicon nitride, and boron nitride, have also been produced. Since there are several types of ceramic fibers, there is also a range of chemical and physical properties. Most fibers are white to cream in color and tend to be polycrystallines or polycrystalline metal oxides (Figure 2.5).

Continuous ceramic fibers present an attractive package of properties. They combine rather high strength and elastic modulus with high-temperature capability and a general freedom from environmental attack. These characteristics make them attractive as reinforcements in high-temperature structural materials. There are three ceramic fiber fabrication methods: chemical vapor deposition, polymer pyrolysis, and sol-gel techniques.

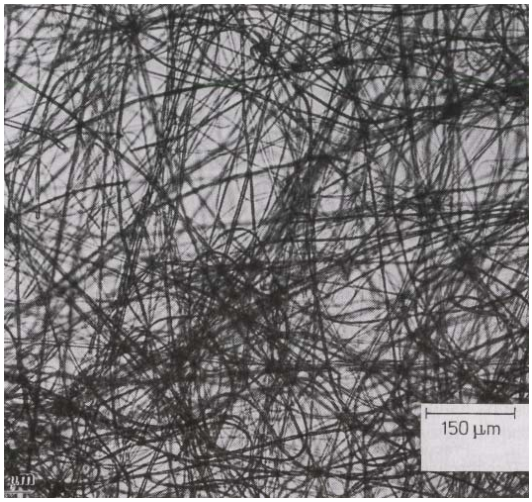


Figure 2.5 Optical micrograph of ceramic fiber (Chawla, 1998).

Ceramic fibers are used as insulation materials and are significant replacements for asbestos. Due to their ability to withstand high temperatures, they are used primarily for lining furnaces and kilns. Their light weight, thermal shock resistance, and strength make them useful in a number of industries. High-temperature resistant ceramic blankets and boards are used in shipbuilding as insulation to prevent the spread of fires and for general heat containment. Ceramic textile products, such as yarns and fabrics, are used extensively in such end-products as heat resistant clothing, flame curtains for furnace openings, thermocoupling and electrical insulation, gasket and wrapping insulation, coverings for induction-heating furnace coils, cable and wire insulation, infrared radiation diffusers, insulation for fuel lines and high pressure portable flange covers. Fibers that are coated with Teflon® are used as sewing threads for manufacturing high-temperature insulation shapes for aircraft and space vehicles. The spaces between the rigid tiles on space shuttles are packed with this fiber in tape form.

2.2.2.4 Glass Fibers

Common glass fibers are silica based (~50-60% SiO_2) and contain a host of other oxides (calcium, boron, sodium, aluminum, iron etc.). Table 2.2 gives the composition of some commonly used glass fibers. The designation *E* stands for electrical because E glass is good electrical insulator in addition to having good

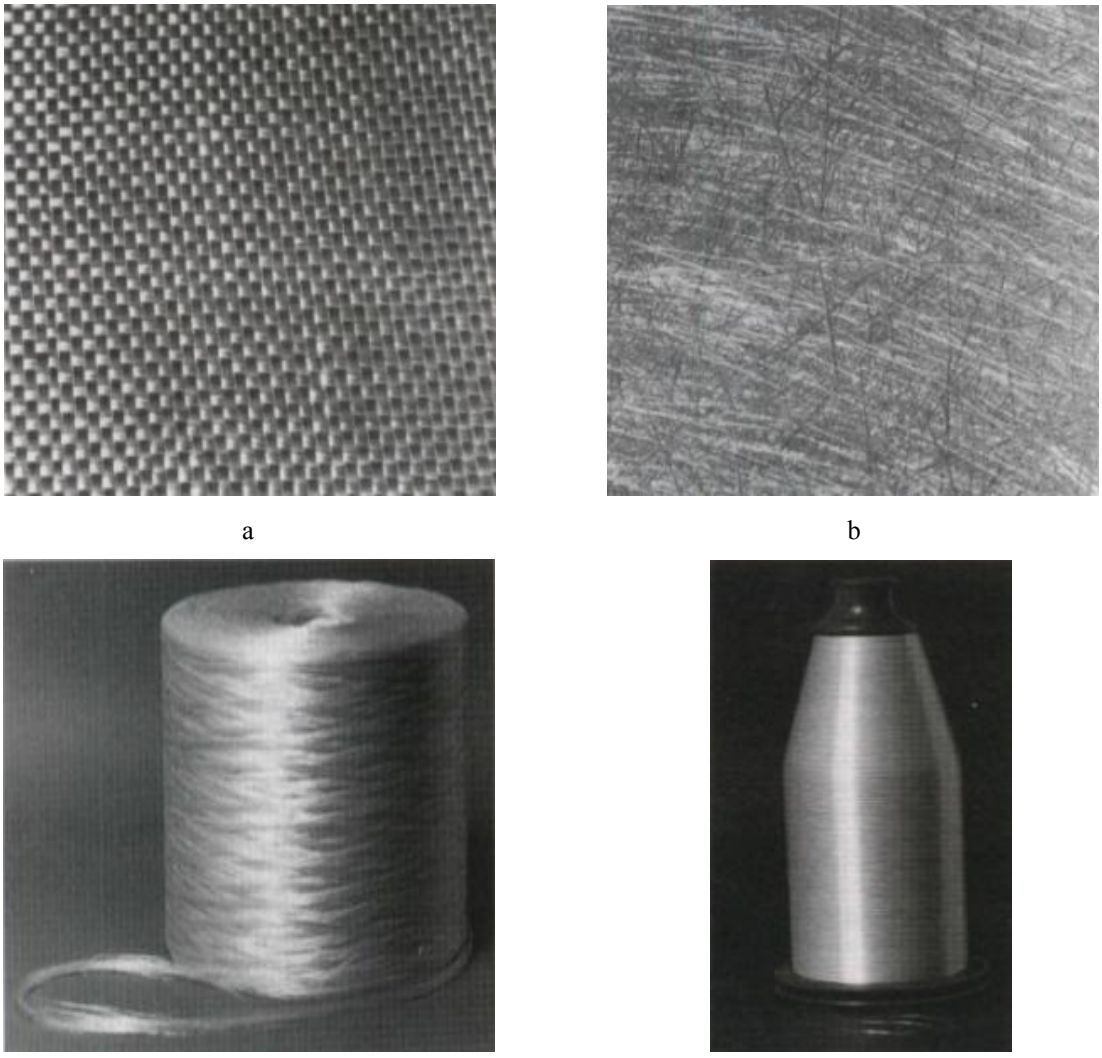
strength and a reasonable Young's modulus; C stands for corrosion because C glass has a better resistance to chemical corrosion; S stands for the high silica content that makes S glass withstand higher temperatures than other types of glasses.

Table 2.2 Approximate chemical compositions of some glass fibers (Chawla, 1998).

Composition	E Glass	C Glass	S Glass
SiO_2	55.2	65	65
Al_2O_3	8	4	25
CaO	18.7	14	–
MgO	4.6	3	10
Na_2O	0.3	8.5	0.3
K_2O	0.2	–	–
B_2O_3	7.3	5	–

Glass fibers are produced by two methods, milling and chopping. The milled fibers are milled using a hammer mill which results in a relatively broad (but consistent) length distribution. The diameter depends on the filament diameter manufactured for milling process. The chopped fibers are produced by chopping a bundle of glass filaments to a precise length. The length of chopped fibers is substantially larger than that of the milled fibers. In both cases, fibers may or may not contain sizing or surface modification. If sizing is applied, it is optimized for a certain type or types of polymers. Cationic sized milled fiber is suggested for polyester epoxy, phenolic and thermoplastics. Silane modified grades are for urethanes and thermoplastics, and glass fiber without any sizing agent is suggested for use in PTFE (Poly Tetra Fluoro Ethylene) and thermoplastics (Wypych, 2000).

Glass fibers are extensively used by industry for reinforcement of polyester, epoxy, and phenolic resins and for the improvements they produce in thermal properties such as reduction in thermal expansion and increase in heat deflection temperature. Moisture decreases glass fiber strength and they are also susceptible to static fatigue. Available glass fiber forms are given in Figure 2.6.



a b

c d

Figure 2.6 Available glass fiber forms; fabric (a), chopped strand (b), roving (c), continuous yarn (d) (Chawla, 1998).

2.2.2.5 Organic Fibers

In general polymeric chains assume a random coil configuration; therefore the molecular chains are neither aligned in one direction nor stretched out. Thus, they have predominantly weak van der Waals interactions rather than strong covalent interactions, resulting in a low strength and stiffness. However, if oriented molecular chains are obtained and packed in parallel, strong and stiff polymers can be produced. Natural organic fibers such as cellulose or synthetic organic fibers can be used in composite materials. Two very different approaches have been taken to make high-modulus synthetic organic fibers. These are:

1. Processing the conventional flexible-chain polymers in such a way that the internal structure takes a highly oriented and extended-chain arrangement. Structural modification of "conventional" polymers such as high-modulus polyethylene was developed by choosing appropriate molecular weight distributions, followed by drawing at suitable temperatures to convert the original folded-chain structure into an oriented, extended chain structure.

2. The second, radically different, approach involves synthesis, followed by extrusion of a new class of polymers, called liquid crystal polymers. These have a rigid rod molecular chain structure. The liquid crystalline state, as we shall see, has played a very significant role in providing highly ordered, extended chain fibers.

These two approaches have resulted in two commercialized high-strength and high-stiffness fibers, polyethylene and aramid.

2.2.2.5.1 Cellulose Fibers

Cellulose fibers offer many valuable properties but the most important characteristic is that they are natural in origin. They are safe to use, non-polluting, and energy efficient. These qualities are the major reasons for the growing interest in these fibers. Technical cellulose fibers are produced by recycling of newsprint, magazines, and other paper products. There are also numerous industrial applications for these fibers which exploit their chemical functionality (reactivity) for crosslinking, their ability to retain water and their hydrogen bonding capability for improvement of rheological properties. The shape of fiber helps to prevent cracking, reduce shrinkage, increase green strength, and reinforce materials.

Virgin fibers produced from wood pulp contain 99.6% cellulose and they are white. Fibers manufactured from reclaimed materials contain 75% and they are gray

or brown (Wypych, 2000). Cellulose fibers (especially virgin materials) have a complex morphological structure which facilitates reinforcement (Figure 2.7).



Figure 2.7 The morphology of cellulose fibers (Wypych, 2000).

2.2.2.5.2 Oriented Polyethylene Fibers

Polyethylene is the most popular plastic in the world. This is the polymer that makes grocery bags, shampoo bottles, children's toys, and even bullet proof vests. For such a versatile material, it has a very simple structure, the simplest of all commercial polymers. A molecule of polyethylene is nothing more than a long chain of carbon atoms with two hydrogen atoms attached to each carbon atom (Figure2.8). The chain of carbon atoms may be many thousands of atoms long.

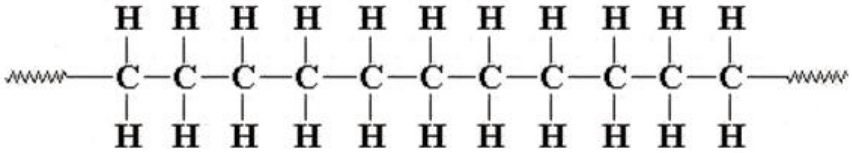


Figure 2.8 The molecule of polyethylene.

The ultrahigh molecular weight polyethylene fiber is a highly crystalline fiber with very high stiffness and strength. This results from some innovative processing and control of the structure of polyethylene. The unit cell of a single crystal

(orthorhombic) of polyethylene has the dimensions of 0.741, 0.494, and 0.255 nm (Chawla, 1998). There are four carbon and eight hydrogen atoms per unit cell. Its strength and modulus are slightly lower than those of aramid fibers but on a per-unit-weight basis, specific property values are about 30% to 40% higher than those of aramid. As is true of most organic fibers, both polyethylene and aramid fibers must be limited to low-temperature (lower than 150°C) applications. High-modulus polyethylene fibers are hard to bond with any polymeric matrix. Some kind of surface treatment must be given to the polyethylene fiber to bond with resins such as epoxy and (PMMA). Photomicrographs of polyethylene fibers are given in Figure 2.9.

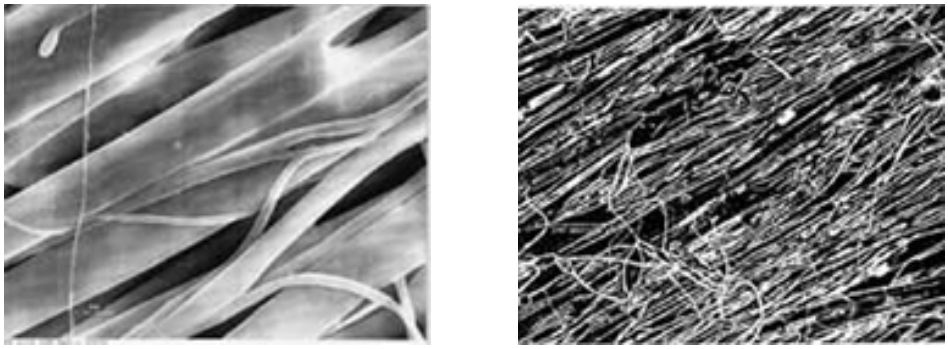
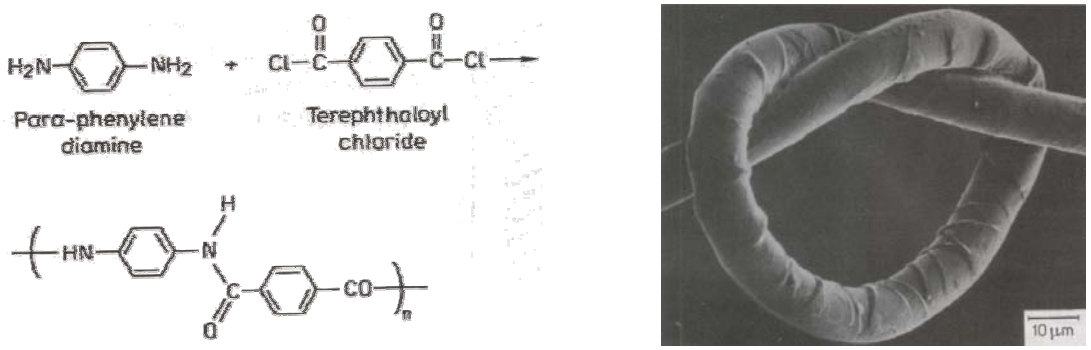


Figure 2.9 Photomicrographs of polyethylene fibers (Wypych, 2000).

2.2.2.5.3 Aramid Fibers

Aramid fiber is a generic term for a class of synthetic organic fibers called aromatic polyamide fibers. The U.S. Federal Trade Commission gives a good definition of an aramid fiber as “a manufactured fiber in which the fiber-forming substance is a long-chain synthetic polyamide in which at least 85% of the amide linkages are attached directly to two aromatic rings”. The basic chemical structure of aramid fibers consists of oriented para-substituted aromatic units, which make them rigid rodlike polymers (Figure 2.10). The rigid rodlike structure results in a high glass transition temperature and poor solubility, which makes fabrication of these polymers, by conventional techniques, difficult.



a b

Figure 2.10 Chemical structure of aramid fiber (a), knotted Kevlar aramid fiber (b) (Chawla, 1998).

They have been in use for a long time to improve wear resistance of plastic parts. Aramid fiber is superior to other wear resistant additives due to its easier dispersion and minimal effect on mechanical properties of filled materials. Incorporation of fibers increases the impact strength of composites. Further improvements in mechanical properties can be obtained by modification of the surface with OH and COOH groups. The presence of these groups was found to increase adhesion to many polymers. The degree of modification should be carefully controlled because the mechanical strength of the fiber and the performance of its composite may be adversely affected (Wypych, 2000). The high moisture absorption of aramid fibers is their biggest disadvantage. It was reported in the literature that moisture absorption by epoxy laminates degrades their mechanical properties. Hygroscopic fibers provide an easy route for moisture ingress. The addition of aramid fibers to epoxy and phenolic composites slightly improves their flame resistance and decreases smoke formation. This fiber also has a high resistance to shock loading and a low density, these two factors combined promote its use in bulletproof clothing.

2.2.2.6 Whiskers

Whiskers are monocrystalline short fibers with extremely high strength. This high strength is because of the absence of crystalline imperfections such as dislocations and having no grain boundaries. Typically whiskers have a diameter of a few μm and a length of a few mm (Figure 2.11). thus their aspect ratio (length/diameter) can vary from 50 to 10000. Whiskers do not have uniform dimensions or properties. This is perhaps their greatest disadvantage. Handling and alignment of whiskers in a matrix to produce a composite is another problem.

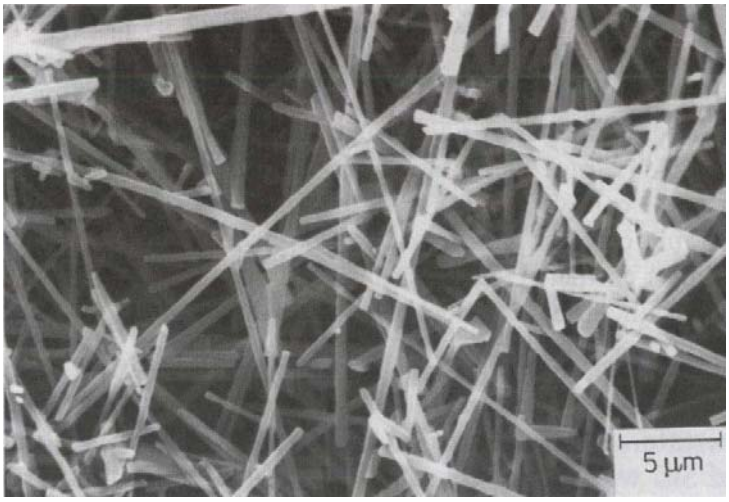


Figure 2.11 Scanning electron micrograph of SiC whiskers (Chawla, 1998).

CHAPTER THREE
THERMAL EXPANSION BEHAVIOUR OF FIBER REINFORCED COMPOSITES

3.1 Coefficient of Thermal Expansion (CTE)

An increase in temperature causes the vibrational amplitude of the atoms in the crystal lattice of the solid to increase. Therefore the average spacing between the atoms increases, causing the material to expand. If the temperature change, ΔT, is such that the material does not go through a phase change, then the coefficient of volumetric thermal expansion (α_v) (Callister, 1994) of a material is defined as

$$\alpha_v = \frac{1}{V}\left(\frac{\partial V}{\partial T}\right) \tag{3.1}$$

where V is the total volume of the material. If we consider one dimension only, we obtain the coefficient of linear thermal expansion (α_l) as

$$\alpha_l = \frac{1}{l}\left(\frac{\partial l}{\partial T}\right) \tag{3.2}$$

where l is the total length of the body. If the length increases approximately linearly with the temperature in the temperature range observed and

$$\Delta l = l - l_0 \tag{3.3}$$

is small when compared with the initial length l_0, then coefficient of linear thermal expansion can be written as

$$\alpha_l = \frac{\Delta l}{l_0} \cdot \frac{1}{\Delta T} \tag{3.4}$$

3.2 Factors Affecting the Coefficient of Thermal Expansion

Factors affecting the thermal expansion coefficient of composite materials are: fiber and void volumes, lay-up angle, thermal cycling, temperature dependence, moisture effects and material viscoelasticity.

3.2.1 Fiber Volume

The dependence of fiber volume is illustrated in Figure 3.1 for a unidirectional lamina consisting of glass fibers dispersed in an epoxy matrix. These curves were calculated based on formulas given by Shapery (1968). As seen in Figure 3.1, at approximately 60 percent fiber content, the longitudinal coefficient of expansion (CTE) is unaffected by any changes in the laminate fiber content. In the case of transverse CTE, the sensitivity is more pronounced. For the angle ply laminates comprised of several layers, the effect of fiber volume on the thermal expansion behavior of the laminate may not be negligible.

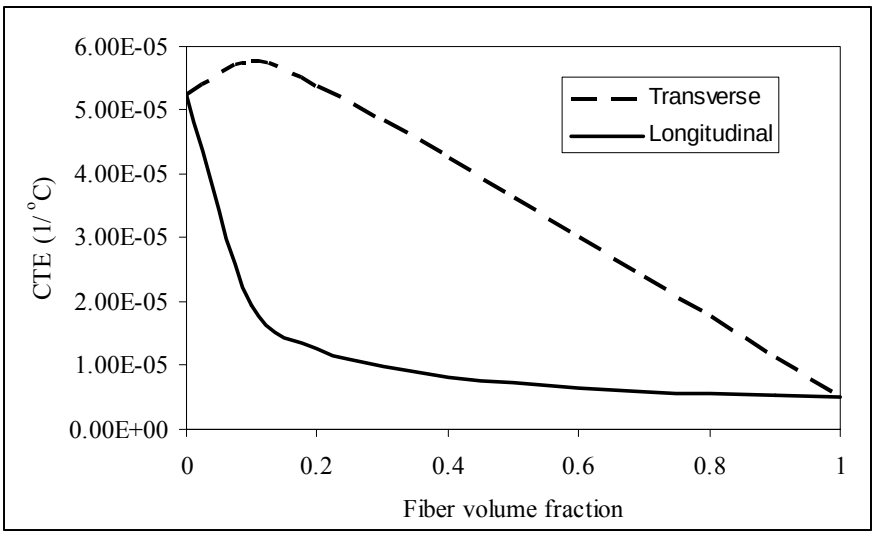


Figure 3.1 Variation of CTE of an epoxy-glass fiber lamina with fiber content of 60%.

3.2.2 Void Volume

The direct effect of voids on the CTE of composites is small within the bounds of practical manufacturing requirements (1.5 percent max. void volume) (Johnson, R.R., Kural M.H., & Mackey G.B. 1981). However the presence of voids can indirectly affect the CTE of a composite by initiating microcracks in the matrix. Voids in the matrix also tend to increase the potential moisture content of the matrix.

3.2.3 Lay-up Angle

One of the main advantages of laminated fiber reinforced composites is that mechanical and thermal response of composites can be tailored directionally to satisfy design requirements. This is accomplished by varying the orientation of each layer in a systematic manner to reach the desired effect. Figure 3.2 shows the variation of CTE of unidirectional composites with fiber orientation.

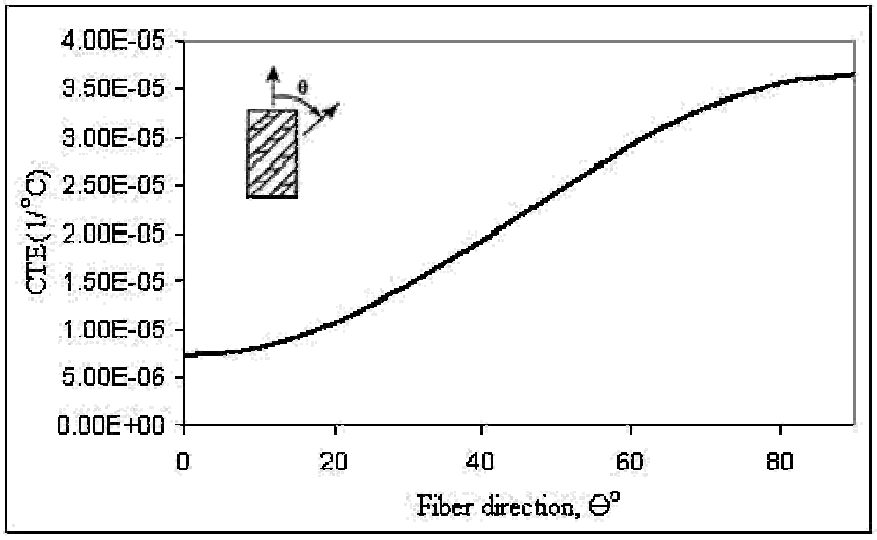


Figure 3.2 Variation of CTE of composite with fiber orientation.

The sensitivity of the composite CTE to variations of fiber orientations can be severe. Although manufacturing tolerances for the lay-up angles are typically $\pm 3^{o}$, this practice can lead to serious CTE deviations for dimensionally critical structures (Johnson, R.R. et al. 1981).

3.2.4 Thermal Cycling

The primary influence of thermal cycling on CTE of composites is to induce matrix microcracking. When microcracking occurs composite becomes partially decoupled. Matrix degradation proceeds gradually at first, and then somewhat more rapidly, and can be detected by changes in the composite thermal response. Therefore CTE of the composite changes. This drift depends on many factors including materials, rate and number of thermal cycles, temperature extremes, and mechanical load level and lay-up angle.

3.2.5 Temperature Dependence

It is a common way to report the CTE of materials as a single quantity and these values are often used by designers and analysts in the same manner. This practice may precipitate significant errors in composite design because of the temperature dependence of the thermal expansion behavior of composite materials. This temperature dependence is mainly caused by the mechanical and physical changes in the resin system. The CTE is a calculated value which is the slope of the thermal strain-temperature curve between two temperature and the CTE values should be obtained from thermal expansion test data for the specific design temperature.

3.2.6 Moisture Effects

The dimensional stability of composites is highly affected by exposure to complex hygrothermal histories. Moisture causes swelling and plasticization of the resin system. The swelling phenomenon alters internal stresses, thus causing a dimensional change in the laminate. Coupled with plasticization of the resin system, permanent dimensional changes up to 30 percent have been observed in laboratory experiments after exposure to complex hygrothermal histories. Dimensional changes caused by a temperature change are much less than the dimensional change due to moisture exposure. It is therefore important to account for moisture effects in assessing dimensional changes due to thermal effects.

3.2.7 Viscoelasticty

Changes in the internal stresses due to moisture and thermal environment can result in significant dimensional changes in composites. Internal stress levels also change due to the viscoelastic phenomenon called the relaxation of the matrix. Actually, relaxation of the internal stresses is a continuous process even without any mechanical, thermal or moisture excursions. This process is usually minimized by placing fibers in the direction where dimensional stability is required.

3.3 Thermal Expansion Measurement Techniques

Thermal expansion measurements can be made by mechanical dilatometry, optical interferometry, or strain gauging methods. Each method has its strengths and limitations in terms of quality of data, repeatability and calibration issues. Factors affecting the results are internal stress distributions in the composites themselves, applied forces, and the representative nature of the volume of material being sampled by the technique.

One of the key points arising from an experimental study by Morrell (1997) is the importance of the composite test-piece having a representative volume. Interruption of the reinforcement by cutting free surfaces influences the internal stresses, and this can influence the recorded thermal expansion data. The test-piece therefore needs to be large enough that the reinforcement can be considered substantially homogeneous and that effects of the cut edges and the local inhomogeneities can be ignored. For in-plane measurements on continuous fiber polymer matrix composites it is preferred to use a square plate test-piece. The effect is not thought to be significant in homogeneous particulate reinforced materials. Further, in long-fiber multi-ply materials it seems to be important to ensure that the through-thickness structure is symmetrical, so that no bending occurs. Normally, composites are designed with symmetrical lay-ups to prevent this, but manufacturing processes do not always guarantee perfect balance. Machining test-pieces to a less than normal thickness will unbalance the structure, and could lead to bending during thermal cycling.

3.3.1 Mechanical Dilatometry

This is a well established technique and commercial equipment is readily available. A test piece in bar form is held against a stop in a support tube, and its free end is contacted by a push road. As the test-piece is heated or cooled, its changes in length are transmitted by the push-rod to a measurement device, usually a displacement transducer.

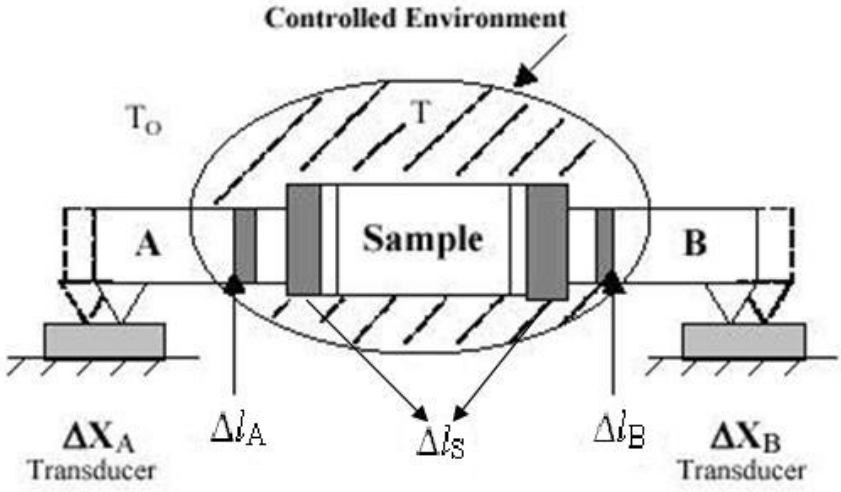


Figure 3.3 Operation principle of a mechanical dilatometer (http://www.anter.com/TN69.htm).

In principle, one can devise a simple arrangement in which the movement is transmitted out of the controlled environments and into the ambient by holding the sample between two rods which extend outside of the heated region as shown on Figure 3.3. The sample pushes the two rods (A and B) as it is being heated, and will expand an amount shown by the shaded area called sample displacement, Δl_S. By examining the experimental model, it becomes immediately clear that this configuration will not produce the desired Δl_S on transducers. Since portions of both rods A and B are in the controlled environment, it is inevitable that they themselves will also expand (Δl_A and Δl_B respectively). Thus, the measured value of transducer displacement ($\Delta X_A+\Delta X_B$) will contain ($\Delta l_A+\Delta l_B$) in addition to Δl_S. The sample's length change, Δl_S, can therefore be written as:

$$\Delta l_s = \left(\Delta X_A - \Delta l_A\right) + \left(\Delta X_B - \Delta l_B\right) \tag{3.5}$$

Unless values of Δl_A and Δl_B are assigned, the true magnitude of Δl_S cannot be determined from the measured values of ΔX_A and ΔX_B alone. Obviously, if Δl_A and Δl_B are not present at all, the measurement becomes absolute, but as long as this is not the case, the measurement is, in principle, a relative one.

Calibration routines are also well established, and have been incorporated into standards. The key factors in calibration are the absolute sensitivity of the displacement measuring device, the temperature homogeneity of the system, which can lead to a "baseline" shift (positive or negative apparent displacements with no test-piece present), and the correction for the expansion of the apparatus itself which the test-piece's length is compared against. It is necessary to set up a calibration procedure to identify these factors, to ensure that they are consistent and to use them to correct the direct output for an unknown to the true thermal expansion behavior. There are several options for doing this. One possibility is to run the apparatus with two very different reference materials for which the expansion data are known. The difference in output is then directly related to the difference in responses of the apparatus for the two materials. The actual output of either reference material, but usually the one with characteristics closest to those of the apparatus material itself, can be used to obtain the apparatus expansion characteristic. Other ways to calibrate the sensitivity of the measuring device are directly using a micrometer for displacing it to known amounts, to run the apparatus with no test-piece to obtain the baseline shift and to use a single reference material to determine the correction for the apparatus expansion. In either case, the reproducibility and reliability of the calibrations have limitations imposed primarily by the repeatability of mechanical contacts between the test-piece or reference pieces and the apparatus, which in turn relates to how the test-piece is held in the apparatus, and the conditions of its end contacts. These limitations are generally poorly understood, and lead to the quotation of results to unwarranted numbers of significant figures.

Typically, a mechanical dilatometer operated with care and attention to repeatability of calibrations and measurement procedures can achieve a reproducibility of about $\pm 0.2 \times 10^{-6}\ K^{-1}$ measured over a range of 100 K, with an

absolute accuracy of about ± 0.2 x 10^{-6} K^{-1}. Thus over large temperature ranges, the absolute accuracy can be better than this, and over smaller temperature ranges, rather worse. The accuracy is best treated in this manner, because the limiting mechanical instabilities are present whatever the expansion coefficient of the material, and the sensitivity factor (a single temperature independent figure) can usually be determined rather more accurately than the other temperature dependent factors (Morrell, R. 1997).

The push-rod in a mechanical dilatometer normally applies a compressive axial force on the test-piece to maintain constant contact. Typically this force is 0.5 – 2 N, but may be less if a balanced thermomechanical analyzer type of apparatus is used. This force may be sufficient to induce permanent distortion in composites when the matrix phase softens. In polymer-based systems, this can happen above 150°C, and in aluminum alloy based metal-matrix composites, above about 450°C. The distortion may be limited to "bedding down" of the contact surfaces, but in some cases, may induce bulk creep effects. The progressive "ratcheting" seen in repeat thermal cycling of some composites may in part be attributable to creep effects. The effects tend to be negligible parallel to the reinforcement directions in long-fiber composites, but may be considerable across ply structures in 2D laminates (Morrell, R. 1997).

3.3.2 Interferometry

This is a potentially much more accurate method for determining thermal expansion. A coherent light source is split and reflected off surfaces at each end of the test-piece, and then recombined. As the test-piece expands, the level of interference between the recombined beams changes, and the total expansion can be determined by counting the number of dark fringes detected. One fringe corresponds to a test-piece end-face relative displacement of l/4. For a calibrated wavelength, the method is potentially absolute, and needs no correction factors. Displacements as small as l/1000 can be resolved with certain types of interferometer (Morrell, R. 1997). However, the quality of the test-piece surfaces is a key issue. They normally

need to be optically flat and reflective to act as their own mirrors. If this is impossible, as is usually the case with composite materials, mirrors need to be placed on the end surfaces, which poses questions of mechanical stability and correction for the expansion of the mirrors. Figure 3.4 illustrates the basic features of a Michelson laser interferometer.

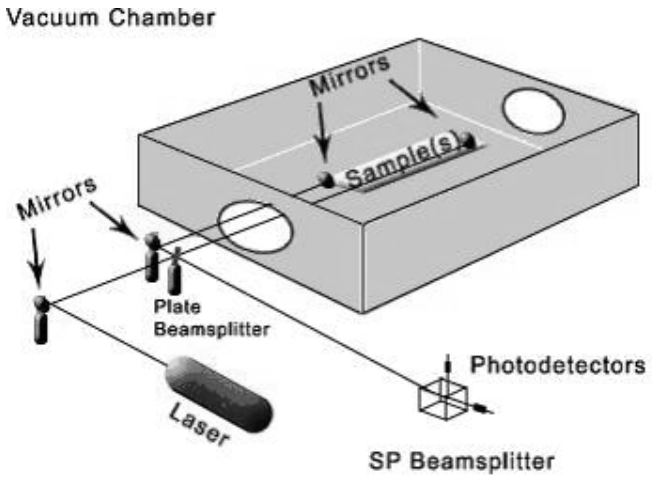


Figure 3.4 Basic illustration of the Michelson laser (http://www.pmiclab.com/index.html).

Other factors requiring consideration are alignment of the mirrors, temperature homogeneity of the test-piece and the temperature stability needed to obtain stable fringes. In addition, the measurement normally has to be conducted in vacuum to avoid the distorting effects of convection in air along the beam path. The technique is best suited to accurate measurements near room temperature, particularly on low thermal expansion materials.

Separate mirrors have to be used because composites cannot be adequately polished to give reflective surfaces. Resting the test-piece stably on a mirror and placing a second mirror on the top surface is the simplest configuration to use. The test-piece surfaces need to be accurately flat and parallel, and moulded surfaces may have to be machined to achieve the alignment conditions required for the mirrors. Care is needed not to unbalance systems in such a machining process. Typically, test-pieces might be quite small, but for larger items made from low thermal expansion materials, carefully aligned mirrors can be glued to a face of the composite in order to achieve representative lengths to measure expansion.

3.3.3 Strain Gauges

This relatively little-used technique has been evaluated on composite materials and found to be quite promising provided care is taken over calibration routines (Morrell, R. 1997). The technique used employs a thermal expansion reference material with an identical strain gauge attached to it and wired so that the differential expansion is recorded. There are considerable advantages in this technique for examining the spatial homogeneity of expansion or dimensional stability of large pieces inappropriate for dilatometry or interferometry. The main drawback is the temperature limitation of the gauge and the means of securing it to the material. Conventional foil gauges can be used typically to 200°C, and although higher-temperature versions and appropriate adhesives can be obtained, they are relatively expensive and specialized, so that 200°C should be taken as the upper temperature limit.

It is essential that identical installation techniques are employed on the test-piece and on the reference, and that the reference is well characterized over the required temperature range. In the tests they must also be at identical temperatures, and thus this technique should ideally to be performed at a series of temperature holds with stabilization periods, unless the test-pieces have sufficiently small thermal masses that the test can be done reliably during temperature ramping.

The technique had been validated using copper and aluminum with ULE silica (Corning Glass Works, near zero expansion coefficient glass) as the zero reference (Morrell, R. 1997). Questions of the lateral sensitivity of strain gauges do not apply to isotropic materials as the test-pieces are not mechanically strained, and any secondary effects are eliminated in the difference calculations. Comparisons between mechanical dilatometry and the strain gauge technique had been carried out on metal matrix composites by Morrell (1997), and a good match was found to 200°C, above which the properties of the gauge and/or its adhesive affected the results. With anisotropic materials, lateral sensitivity is more important, and increases the potential errors in the results.

The area covered by a strain gauge is usually quite small, 1-5 mm, and this means that it samples the local behavior rather than the longer range average. In composites which have homogeneous reinforcement, such as flat laminates, unidirectional reinforcements and particulate composites, the technique can be used reliably, but caution needs to be exercised with woven structures. The active part of the strain gauge needs to cover several representative reinforcement units for the results to be representative of bulk material behavior.

3.4 Theoretical Consideration

Micromechanics is a study of mechanical properties of composites in terms of those of constituent materials (Tsai, & Hahn 1980). In discussing composite properties it is important to define a volume element which is small enough to show the microscopic structural details, yet large enough to represent the overall behavior of the composite. Such a volume element is called the representative volume element. A simple representative volume element can consist of a fiber embedded in matrix block.

Once a representative volume element is chosen, proper boundary conditions are prescribed. Ideally, these boundary conditions must represent the in situ states of stress and strain within the composite. That is, the prescribed boundary conditions must be the same as those if the representative volume element were actually in the composite.

Finally, a prediction of composite properties follows from the solution of the forgoing boundary value problem. Although the procedure involved is conceptually simple, the actual solution is rather difficult. Consequently, many assumptions and approximations have been introduced, and therefore, various solutions are available.

General assumptions in micromechanics of composites are:

- The composite is macroscopically homogeneous and orthotropic, linearly elastic, initially stress free, and free of voids. There is complete bonding at the interface of the constituents and there is no transitional region between them. The displacements are continuous across the fiber matrix interphase (there is no interfacial slip).
- The fibers are homogeneous, linearly elastic, isotropic or orthotropic, regularly spaced, perfectly aligned, circular in cross section, and infinitely long in the longitudinal direction.
- The matrix is homogeneous, linearly elastic, and isotropic.
- The temperature is uniform and remains uniform during the temperature increase. Constituent material properties do not vary with temperature.

3.4.1 Some of the Existing Theories

Consider a random two-phase composite. Assuming that one of the phases, subscript *f*, is dispersed in a polymer phase, subscript *m*, and $\alpha_m > \alpha_f$, where α is the thermal expansion coefficient of the phases. When such a composite is heated, even under conditions of no external loading, the matrix will wish to expand more than the fillers and if the interface is capable of transmitting the stresses which are set up as a result of differences between the thermal expansion coefficients and elastic constants of the constituents so that the expansion of the matrix will be reduced. These thermal stresses cause stress concentrations which may initiate yielding or debonding. Therefore, in design analysis, it is important to understand how these stresses arise and how to control the thermal expansion coefficients of the composite. In the theoretical treatments to be described, except for the equations of Sideridis (1994), it is assumed that the adhesion at the interface is adequate to withstand this task.

3.4.1.1 Law of Mixtures

If each phase is assumed homogeneous and isotropic and linearly elastic over a small range of volumetric strains, in the absence of the phase interaction, one may

expect the coefficient of thermal expansion of a composite to follow simple law of mixtures given by:

$$\alpha_c = \alpha_f \upsilon_f + \alpha_m \upsilon_m \tag{3.6}$$

where α_c, α_f, α_m are thermal expansion coefficients of the composite, filler and matrix respectively and υ_f and υ_m are the volumetric fractions of the filler and the matrix.

Because of the differences in the thermal expansivities of the phases a state of micro-stress often exists between them. These stresses influence the thermal expansion behavior of the body. Thus, its thermal expansion coefficient does not follow the rule of mixtures.

3.4.1.2 Equation of Thomas

Thomas (Sideridis, 1994) put forward an empirical solution which can be written as

$$\alpha_c^a = \alpha_f^a \upsilon_f + \alpha_m^a \upsilon_m \tag{3.7}$$

where *a* may vary from -1 to +1, and γ is the volumetric thermal expansion coefficient which is defined as $\alpha_c = 3\alpha$ for an isotropic composite. However, for a unidirectional composite, which is isotropic in the two transverse directions, the relation between volumetric thermal expansion coefficient and longitudinal and transverse thermal expansion coefficients can be written as

$$\alpha_c = \alpha_1 + 2\alpha_2 \tag{3.8}$$

where α_1 is the thermal expansion coefficient in the longitudinal direction and α_2 is the thermal expansion coefficient in the transverse direction. The empirical nature of the equation makes it suitable for most filed systems by the correct use of the adjustable constant.

3.4.1.3 Equation of Van Fo Fy

In a series of articles by Van Fo Fy (1965), thermal expansion coefficients for matrices reinforced by continuous fibers are developed by means of a detailed stress analysis. As a result of this work, the thermal expansion coefficient in the longitudinal direction (α_1) is

$$\alpha_1 = \alpha_m - (\alpha_m - \alpha_f)\frac{(1+\nu_m)E_f\upsilon_f - (1+\nu_{f12})(E_1 - E_m\upsilon_m)}{(\nu_m - \nu_{f12})E_1} \tag{3.9}$$

and the thermal expansion coefficient in the transverse direction (α_2) is

$$\alpha_2 = \alpha_m + (\alpha_m - \alpha_1)\nu_{12} - (\alpha_m - \alpha_f)(1+\nu_{f12})\frac{\nu_m - \nu_{12}}{\nu_m - \nu_{f12}} \tag{3.10}$$

where E_f, E_m are elastic moduli and ν_f, ν_m are the Poisson's ratios of fiber and matrix respectively. E_1 is the elastic modulus for the longitudinal direction of composite and ν_{12} is the Poisson's ratio of the composite. However, the values predicted by these expressions are very sensitive to variations in E_1 and deviations arose by the experimental error may cause considerable discrepancies. E_1 can be found, using the simple rule of mixtures, as

$$E_1 = E_f\upsilon_f + E_m\upsilon_m \tag{3.11}$$

3.4.1.4 Equation of Cribb

Cribb (Sideridis, 1994) adopted an approach in which no limitations are made on the shape or size of the fillers. The phases are assumed to be homogeneous, isotropic and linearly elastic. The equation is given as

$$\alpha_c = \theta_1\alpha_m + \theta_2\alpha_f \tag{3.12}$$

where

$$\theta_1 = \frac{K_m(K_c - K_f)}{K_c(K_m - K_f)}, \quad \theta_2 = \frac{K_f(K_m - K_c)}{K_c(K_m - K_f)} \tag{3.13}$$

In these equations K_c, K_f and K_m represent the bulk moduli of the composite, filler and matrix respectively. The simplicity of this approach is attractive, but it converts the problem of calculating α_c to knowledge of K_c or an ability to calculate it from the properties and volume fractions of the individual components.

3.4.1.5 Equation of Schapery

Schapery (1968) has derived expressions for the longitudinal and transverse effective thermal expansion coefficients both for isotropic and anisotropic composites consisting of isotropic phases, by employing extremum principles of thermoelasticity.

He considered a specimen under a space wise uniform temperature in the form of a rectangular parallelepiped whose edges are parallel to coordinate axes and with unit volume. This specimen is statistically homogeneous and composed of *n* phases (constituents), each of which has homogeneous mechanical and thermal properties that are different from any other phase. No restriction is placed on the temperature dependence of constituent properties. Maximum dimensions defining the specimen's structural inhomogeneity are assumed small compared to specimen dimensions and the interaction between phases is considered to be purely mechanical and linear. Also specimen and phases are assumed unstressed and unstrained when surface tractions are zero and the temperature is at some reference value.

As a result, for a unidirectional two phase composite, the thermal expansion coefficient in the longitudinal direction is

$$\alpha_1 = \frac{E_f \alpha_f \upsilon_f + E_m \alpha_m \upsilon_m}{E_f \upsilon_f + E_m \upsilon_m} \tag{3.14}$$

and the thermal expansion coefficient in the transverse direction is

$$\alpha_2 = (1+\nu_f)\alpha_f \upsilon_f + (1+\nu_m)\alpha_m \upsilon_m - \alpha_1(\nu_f \upsilon_f + \nu_m \upsilon_m) \tag{3.15}$$

3.4.1.6 Equation of Chamberlain

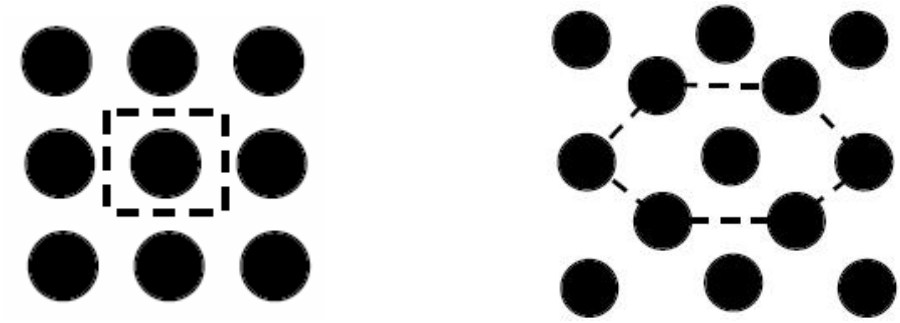
An alternative model for transverse thermal expansion of unidirectional composites was derived by Chamberlain (Rogers et al., 1977), using plane stress thick walled cylinder equations for the case of transversely isotropic fibers in an isotropic matrix. The equation for the longitudinal thermal expansion coefficient is similar to Schapery's formula and can be written as

$$\alpha_1 = \frac{E_{f1}\alpha_{f1}\upsilon_f + E_m\alpha_m\upsilon_m}{E_{f1}\upsilon_f + E_m\upsilon_m} \tag{3.16}$$

where E_{f1} is the elastic modulus of fiber for the longitudinal direction and α_{f1} is the thermal expansion coefficient of fiber in the longitudinal direction. The expression for thermal expansion coefficient in the transverse direction takes the form

$$\alpha_2 = \alpha_m + \frac{2(\alpha_{f2} - \alpha_m)\upsilon_f}{\nu_m(F-1+\upsilon_m) + (F+\upsilon_f) + \frac{E_m}{E_{f1}}(1-\nu_{f12})(F-1+\upsilon_m)} \tag{3.17}$$

where α_{f2} is the thermal expansion coefficient of fiber in the transverse direction, ν_{f12} is the Poisson's ratio of the fiber and F is a packing factor which accounts for fiber packing geometry (Figure 3.5), and is equal to 0.9069 for hexagonal packing and for 0.7854 for square packing respectively.



Square packing Hexagonal packing

Figure 3.5 Idealized fiber packing arrangements.

3.4.1.7 Equation of Rosen and Hashin

Rosen and Hashin (1970) derived expressions for the effective thermal expansion coefficients of multiphase composites and the summary of their approach for unidirectional fiber reinforced composites with transversely isotropic constituents is given as

$$\begin{aligned}\alpha_1 = \hat{\alpha}_1 &+ \left(S_{11} - \hat{S}_{11}\right)\left[(\alpha_{f1} - \alpha_{m1})P_{11} + (\alpha_{f2} - \alpha_{m2})2P_{12}\right] \\ &+ \left(S_{12} - \hat{S}_{12}\right)\left[(\alpha_{f1} - \alpha_{m1})2P_{12} + (\alpha_{f2} - \alpha_{m2})2(P_{22} + P_{23})\right]\end{aligned} \tag{3.18}$$

$$\begin{aligned}\alpha_2 = \hat{\alpha}_2 &+ \left(S_{12} - \hat{S}_{12}\right)\left[(\alpha_{f1} - \alpha_{m1})P_{11} + (\alpha_{f2} - \alpha_{m2})2P_{12}\right] \\ &+ \left(S_{22} - \hat{S}_{22}\right)\left[(\alpha_{f1} - \alpha_{m1})P_{12} + (\alpha_{f2} - \alpha_{m2})(P_{22} + P_{23})\right] \\ &+ \left(S_{23} - \hat{S}_{23}\right)\left[(\alpha_{f1} - \alpha_{m1})P_{12} + (\alpha_{f2} - \alpha_{m2})(P_{23} + P_{33})\right]\end{aligned} \tag{3.19}$$

where

$$\begin{aligned}&S_{11} = \frac{1}{E_1}, S_{22} = S_{33} = \frac{1}{E_2} \\ &S_{12} = S_{13} = \frac{-\nu_{12}}{E_1}, S_{23} = \frac{-\nu_{23}}{E_2}\end{aligned} \tag{3.20}$$

and P_{ab} (a,b=1,2,3) are

$$P_{11} = \frac{A_{22}^2 - A_{23}^2}{\text{Det A}}, P_{13} = P_{12} = \frac{A_{12}A_{23} - A_{12}A_{22}}{\text{Det A}}$$
$$P_{33} = P_{22} = \frac{A_{11}A_{22} - A_{12}^2}{\text{Det A}}, P_{23} = \frac{A_{12}^2 - A_{11}A_{23}}{\text{Det A}} \quad (3.21)$$

where A_{ab} is defined as (S_{fab} - S_{mab}) and Det A is given by

$$\text{Det A} = A_{11}\left(A_{22}^2 - A_{23}^2\right) + 2A_{12}\left(A_{12}A_{23} - A_{12}A_{22}\right) \quad (3.22)$$

In above equations subscripts *f* and *m* refer to fiber and matrix and terms with and without a hat refer to volume average and effective composite properties respectively. S_{ab} can be written for the effective property, the volume average property and the constituent properties. Composite volume average properties are obtained with the expression

$$\hat{p} = p_f \upsilon_f + p_m \upsilon_m \quad (3.23)$$

and composite effective mechanical properties are given by Hashin (1979). It is very difficult to find the coefficients of thermal expansion of a composite using equations of Rosen and Hashin because, to determine composite effective mechanical properties the bulk modulus of the constituents and the composite should be determined.

3.4.1.8 Equation of Schneider

Another consideration was made by Schneider (1971), who assumed a hexagonal arrangement of cylindrical fiber-matrix elements consisting of a fiber surrounded by a cylindrical matrix jacket. The equation for the longitudinal thermal expansion coefficient is identical to Schapery's formula. For the transverse direction he derived the following equation

$$\alpha_2 = \alpha_m - (\alpha_m - \alpha_f)\left[\frac{2(1+\nu_m)(\nu_m^2 - 1)C}{\frac{1+1.1\upsilon_f}{1.1\upsilon_f - 1} - \nu_m + 2\nu_m^2 C} - \frac{\nu_m \frac{E_f}{E_m}}{\frac{1}{C} + \frac{E_f}{E_m}}\right] \tag{3.24}$$

in which

$$C = \frac{1.1\upsilon_f}{1 - 1.1\upsilon_f} \tag{3.25}$$

3.4.1.9 Equation of Chamis

Chamis (1984) has used a simple force balance, or strength of materials, approach to derive expression for both mechanical and thermal properties of unidirectional composites with transversely isotropic fibers. The derived expression for the longitudinal thermal expansion coefficient is again identical to Schapery's formula. The expression for the transverse thermal expansion coefficient is

$$\alpha_2 = \alpha_{f2}\sqrt{\upsilon_f} + \left(1 - \sqrt{\upsilon_f}\right)\left(1 + \upsilon_f \nu_m \frac{E_{f1}}{E_1}\right)\alpha_m \tag{3.26}$$

3.4.1.10 Equation of Sideridis

Sideridis (1994) has calculated the expansion coefficients of the composite using a model which introduces the concept of the boundary interphase. This concept determines the influence of the interphase which depends on the quality of adhesion between fiber and matrix. It has been assumed that the composite has well defined material properties for the fiber and matrix, whereas the interphase material has inhomogeneous properties (thermal expansion coefficient, the elastic modulus and Poisson's ratio) varying from the fiber surface to the matrix. He also made the following assumptions:

- A perfect bonding exists at all surfaces.
- The fiber and the matrix materials carry only tensile stresses.
- The interphase material can only carry shear stresses.

The equation for the longitudinal thermal expansion coefficient is

$$\alpha_1 = \frac{\alpha_f E_f \upsilon_f + \alpha_m E_m \upsilon'_m + \int_{r_f}^{r_i} \alpha_i(r) E_i(r) r \, dr}{E_f \upsilon_f + E_m \upsilon'_m + \frac{2}{r_m^2} \int_{r_f}^{r_i} E_i(r) r \, dr} \tag{3.27}$$

and for the transverse thermal expansion coefficient is

$$\begin{aligned} \alpha_2 = (1+\nu_f)\alpha_f \upsilon_f + (1+\nu_m)\alpha_m \upsilon'_m + \frac{2}{r_m^2} \int_{r_f}^{r_i} (1+\nu_i(r))\alpha_i(r) \, dr \\ - \alpha_1 \nu_f \upsilon_f + \nu_m \upsilon'_m + \frac{2}{r_m^2} \int_{r_f}^{r_i} \nu_i(r) r \, dr \end{aligned} \tag{3.28}$$

where r_f, r_i, r_m are the outer radii of the fiber, the interphase and the matrix circular sections respectively, then the fractions of the respective phases are

$$\upsilon_f = \frac{r_f^2}{r_m^2}, \upsilon_i = \frac{r_i^2 - r_f^2}{r_m^2}, \upsilon'_m = \frac{r_m^2 - r_f^2}{r_m^2} \tag{3.29}$$

with

$$\upsilon'_m = 1 - \upsilon_f - \upsilon_i \tag{3.30}$$

The influence of the mode of variation of the interphase material properties (linear, hyperbolic and parabolic) on the thermal expansion coefficient was studied by Sideridis. However, it is inconvenient to determine the thermal expansion coefficient of a composite using equation of Sideridis, because determination of the

radius of the interphase requires making complicated experiments on the produced samples.

CHAPTER FOUR
FINITE ELEMENT METHOD

4.1 Historical Perspective

The finite element method has become a powerful tool for the numerical solution of a wide range of engineering problems such as steady, transient, linear or nonlinear problems in stress analysis, heat transfer, fluid flow, and electromagnetism. With the advantages in computer technology and computer-aided design systems, complex problems can be modeled with relative ease. Several alternative configurations can be tested on a computer before the first prototype is built. In this method of analysis, a complex region defining a continuum is reduced into simple geometric shapes called finite elements. The material properties and the governing relationships are considered over these elements and expresses in terms of unknown values at element corners. An assembly process, considering the loading and the constraints, results in a set of equations. Solution of these equations gives us the approximate behavior of the continuum.

The origin of the modern finite element method may be traced back to early 1900s, when some investigators approximated and modeled elastic continua using discrete equivalent elastic bars. But basic ideas of the finite element method originated from advances in aircraft structural analysis. In 1941, Hrenikoff presented a solution of elasticity problem using the "frame network method". Courant's paper, which used a piecewise polynomial interpolation over triangular subregions to model torsion problems, appeared in 1943. Turner et al. derived stiffness matrices for truss, beam and other elements and presented their findings in 1956. The term finite element was first coined and used by Clough in 1960 (Chandrupatla, & Belegundu, 2002)(Moaveni, 1999).

In the early 1960s, engineers used the method for approximate solution of problems in stress analysis, fluid flow, heat transfer and other areas. A book by

Argyris in 1955 on energy theorems and matrix methods laid a foundation for further developments in finite element studies. The first book on finite elements by Zienkiewicz and Chung was published in 1967. In the late 1960s and early 1970s, finite element analysis was applied to nonlinear problems and large deformations. Oden's book on nonlinear continua appeared in 1972. Mathematical foundations were laid in the1970s. New element development, convergence studies, and other related areas are in this category. Today, the developments in main frame computers and availability of powerful microcomputers has brought this method within reach of students and engineers working in small industries (Chandrupatla, & Belegundu, 2002).

4.2 Finite Element Analysis Procedure

4.2.1 Geometry Creation

The first step in the finite element analysis procedure is to model the part geometry. There are many ways to define geometry, ranging from two-dimensional drawings to three-dimensional computer-aided design. Computer-aided drafting permits easy generation and editing of two-dimensional geometry. In general, this process involves placing lines, rectangles, arcs, circles, and other basic geometric shapes on a display screen and then moving, rotating, and scaling these shapes to define a part outline. Often, there is a need to describe a part in three dimensions so that it can be more easily understood and converted to a discretized finite-element definition. Wireframe modeling is the simplest approach to graphical display of three-dimensional shapes by definition of part outlines and intersections of surfaces. Unfortunately, these models can be obscure and difficult to visualize. Surface modeling goes one step beyond wireframes by describing the individual surfaces of the model, analogous to stretching a thin fabric over the wireframe model. Solid models provide the most accurate description of part geometry by mathematically describing the interior and exterior of the part (Trantina, & Nimmer, 1994).

No matter how the geometry is created, it must eventually be described discretely in terms of nodal points and elements in order to apply finite-element analysis. For complex parts, this process is usually accomplished by using an automated finite-element mesh generator to represent a part discretely in terms of nodes and elements. In spite of the automated nature of this process, there is often a need to apply engineering analysis judgment. For example, if a shell finite-element model is applied, the engineer must be aware that certain concentrations such as the corners of a box may not be adequately modeled locally with the shell analysis. This is a situation that would require a three-dimensional analysis to define local stresses accurately if that were necessary. Therefore, a significant amount of engineering judgment is required to produce an effective geometric representation of a complex part.

4.2.2 Mesh Creation and Element Selection

Once the overall geometry has been defined it must be divided into elements that are connected to one another at the nodal points. This division of the geometry into a set of elements is referred to as a mesh. Engineering judgment is required to select an appropriate element type, as discussed in the preceding section. Also, engineering judgment is required to determine the mesh density and the number and size of the elements. Coarser meshes result in faster solution times but also limit the accuracy of the analysis. Higher mesh densities should be created in regions where large gradients are expected. Automated meshing routines are available where the user can specify the mesh density.

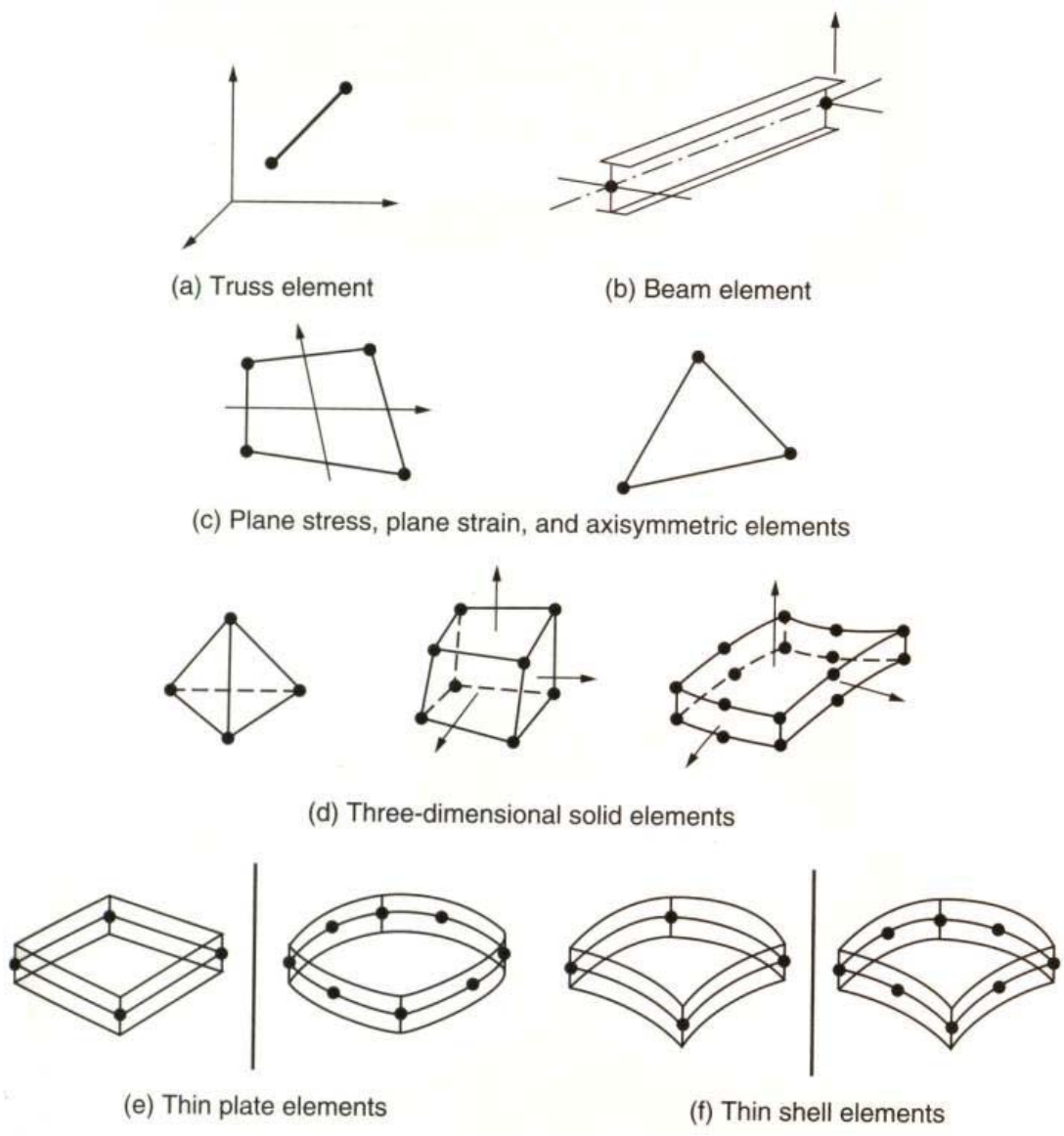


Figure 4.1 Examples of finite elements (Trantina, & Nimmer, 1994).

4.2.3 Boundary and Loading Conditions

Applying boundary conditions and the proper loading on a structure appear as a very important part of the finite element solution. For static problems, the stiffness matrix associated with the linear equations of equilibrium for the complete structure will be singular, unless all rigid body motion is prohibited. As a result, a fundamental requirement for solution of the linear equations governing a problem is that the structure must be prevented from freely translating or rotating in space. Rigid body motion is eliminated through the application of boundary conditions requiring zero

displacements and/or rotations at nodes. Additional displacement boundary conditions can also be applied to the structure to model the actual structural support system. It is not necessary to restrain all of the displacements and rotations at a node. For the thermal analysis problems, prescribed temperatures, conductive heat flux boundary conditions, convection boundary conditions and radiation boundary conditions may be applied to the model.

Loads may be applied to a model either in the form of applied forces, displacements or thermal effects. Concentrated loads can only be applied at the node locations of the elements. Distributed loads and body loads can also be applied to finite-element surfaces and volumes, respectively. Distributed loads are usually internally translated to equivalent nodal loads within the finite-element code.

4.2.4 Defining Material Properties

In addition to the geometric detail of the component and the applied loads, the material (constitutive) properties must also be defined. For simple isotropic, linear-elastic stress analysis, only the material elastic modulus and Poisson's ratio need be provided. In some cases, more detailed constitutive models may be desirable. For example, for highly loaded parts, elastic-plastic behavior may be included. In some cases, properties may be functions of time, rate, temperature, or other variables. It must be emphasized that increased capability in modeling material behavior means in general that more material data must be available. In many cases, such as time-dependent material models, for example, measurements to obtain such data are nonstandard in nature (Trantina, & Nimmer, 1994).

It must be kept in mind that, real material properties are not dependent upon geometry and the property is only useful in the general engineering sense if it is associated with a methodology of applying it to general geometries. Many tests are carried out on materials as functions of rate and temperature to provide comparative performance values. However, in many cases these measurements do not represent true material properties because they are uniquely associated with the test geometry

used to make the measurement and there is no methodology available to generalize the measurement for use in complex geometries.

4.2.5 Displaying Results

After the analyst has defined geometry, element, and node discretization, boundary conditions, loads, and material constitutive relationships, the finite-element code can assemble the equilibrium equations governing the structure. These equations can vary from hundreds to thousands for typical problems. The finite-element code solves this system of equations. As a result of this solution, a massive amount of information is computed displacements of all nodes and stresses, strains, temperatures, heat fluxes etc. in all elements. Fortunately, this information can be displayed with advanced graphics techniques as constant-stress contours or with a color-coded representation of the particular stress range of interest. These results can then be assessed in terms of engineering performance requirements. In order to judge whether failure will occur, material data defining failure limits in terms of stress or strain are generally required.

CHAPTER FIVE
MICROMECHANICAL ANALYSIS BY ANSYS

5.1 Model Development

In the present work, the effective coefficient of thermal expansion (CTE) of different kinds of fiber reinforced composites is studied by micromechanical modeling using finite element method. To determine the both longitudinal and transverse CTEs of composites, three dimensional steady state analyses were undertaken.

Representative unit cell models for different fiber volume fractions and different kind of materials were produced using finite element program ANSYS. The representative unit cell used for the current analysis is a cylinder which is embedded in a cube with unit dimension. Fibers are assumed to have a square packing arrangement. The radius of the cylinder is determined with respect to fiber volume fraction of the composite. Figure 5.1 shows the unit cell considered in the micromechanical analysis. Using the advantage of symmetry, only an octant of the unit cell, indicated in Figure 5.2, is modeled to describe the behavior of the unit cell and of an entire continuum of unit cells for the finite element analysis.

To compare the results of finite element solutions for different types of composites with the results of the analytical methods and to determine the expansion behavior of different material systems with respect to fiber content, models having fiber volume fractions from 10% to 80% with increments of 10% have been composed. Furthermore, comparison between finite element solutions and experimental results have been made upon the models having 40%, 47%, 48%, 54%, 57%, 63%, 65%, and 68% fiber volume fractions.

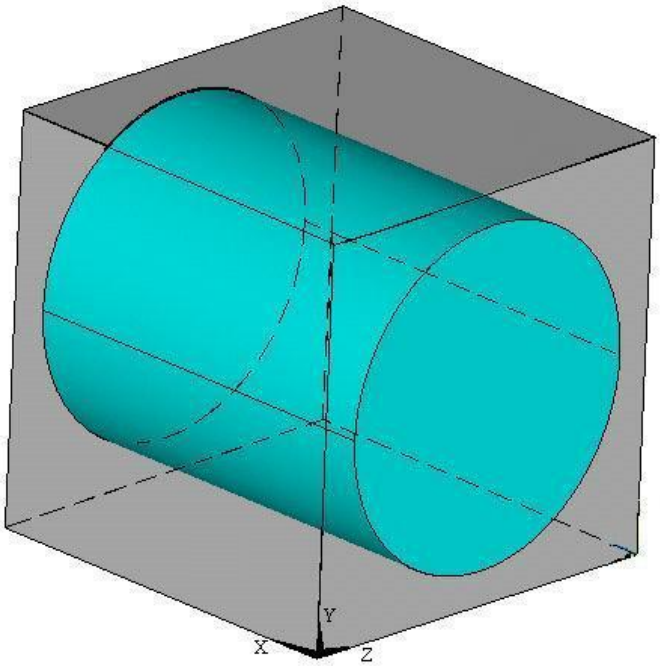


Figure 5.1 A fiber matrix unit cell with a fiber volume fraction of 54%.

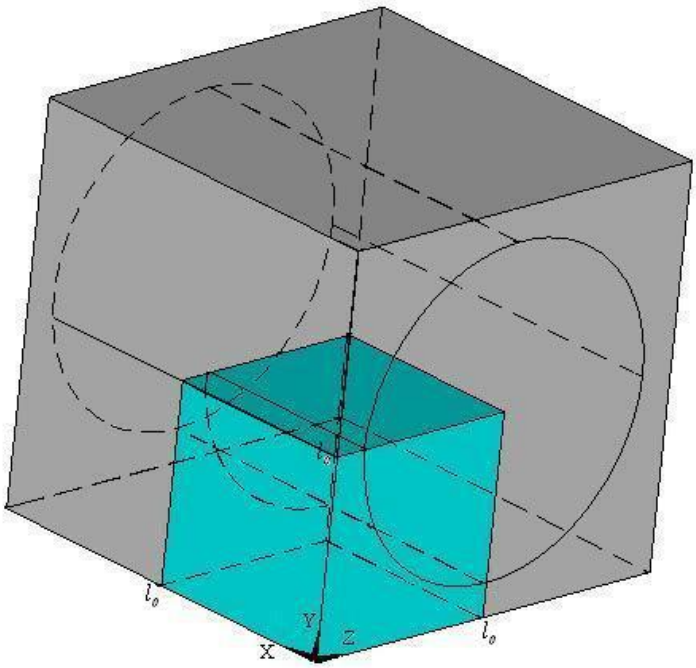


Figure 5.2 Octant of the unit cell which is used for the finite element analysis and its axial (X) and transverse (Y, Z) directions.

5.2 Mesh Creation

10-node tetrahedral coupled field solid element SOLID98 (Figure 5.3) was used for the finite element analyses. The element has a quadratic displacement behavior and is well suited to model irregular meshes. The meshes were made finer in the sharp edges between the boundaries of the model and fiber matrix interface when necessary, especially for the models which have a larger fiber volume fraction than 50%.

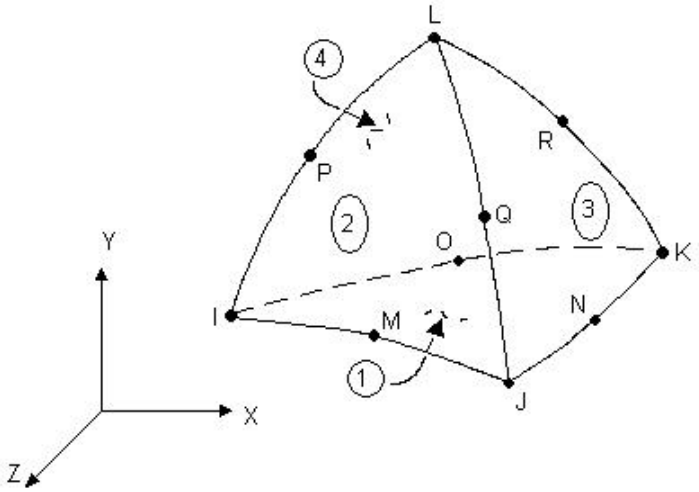


Figure 5.3 The geometry, node locations, and the coordinate system for the element SOLID98.

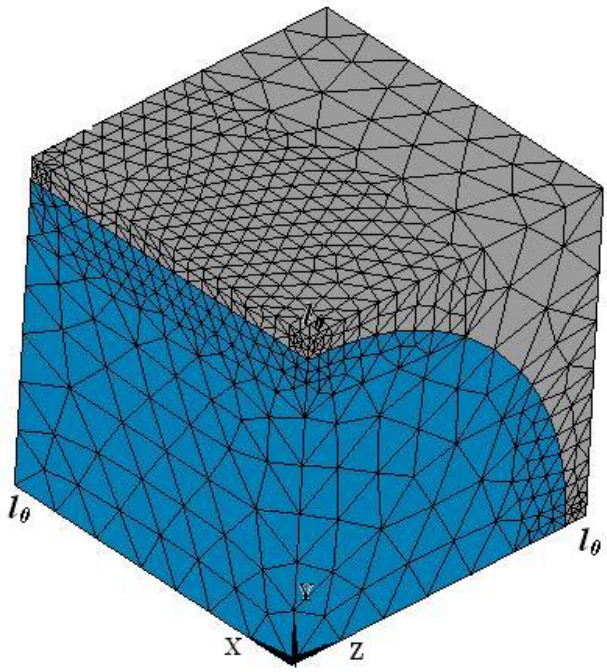


Figure 5.4 A representative meshed unit cell having a fiber volume fraction equal to 68%.

Mesh refinement is performed until the changes in the results are sufficiently small. A representative meshed unit cell having 12678 elements and 19046 nodes is shown in Figure 5.4, and the mesh on the fiber matrix interface is shown in Figure 5.5.

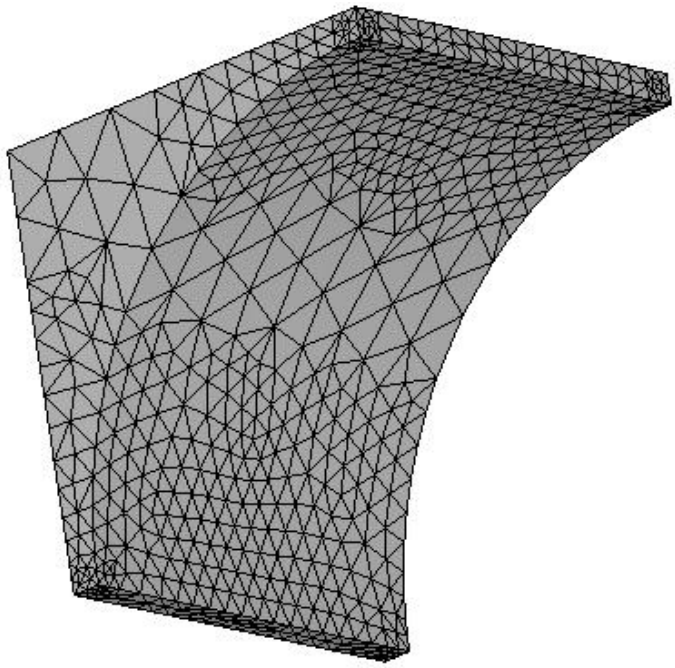


Figure 5.5 The finite element mesh on the fiber matrix interface for fiber volume fraction of 68%.

5.3 Material Properties

The constituent property data used in the analyses are given in Tables 5.1, 5.2, and 5.3. The data in Table 5.1 is taken from the investigation of Sideridis (1994). The unidirectional glass fiber composites used in his investigation consisted of an epoxy matrix (permaglass XE5/1, Permali Ltd, UK) reinforced with long E-glass fibers having a diameter of 0.012 mm. The properties of transversely isotropic carbon fibers and other isotropic matrix materials are taken from the study of Bowles and Tompkins (1989). The constituent properties used in their analyses are given in Table 5.2 and 5.3. Some of these data was experimentally measured values and were taken from various literature sources which include both research papers and manufacturers' product data sheets. However, many of the transverse fiber properties represent values that were calculated from composite properties. T300 and C6000

carbon fibers were assumed to have same properties. All of the epoxies were assumed to have same properties except CE339, which has a larger CTE. This larger value of CTE is due to the rubber particles in this rubber toughened epoxy.

Table 5.1 Material properties, at room temperature, used for the composite consisting of isotropic glass fibers and isotropic epoxy matrix (Sideridis, 1994).

Material	E (GPa)	G (GPa)	ν	α (10^{-6}/ºC)
Epoxy	3.5	3.89	0.35	52.5
Glass fiber	72	40	0.2	5

Table 5.2 Matrix properties at room temperature (Bowles, & Tompkins, 1989).

Matris	E (GPa)	G (GPa)	ν	α (10^{-6}/ºC)
934 epoxy	4.35	1.59	0.37	43.92
5208 epoxy	4.35	1.59	0.37	43.92
930 epoxy	4.35	1.59	0.37	43.92
CE339 epoxy	4.35	1.59	0.37	63.36
PMR15 polymide	3.45	1.31	0.35	36
2024 Aluminum	73.11	27.58	0.33	23.22
Borosilicate glass	62.76	26.20	0.20	3.24

Table 5.3 Carbon fiber properties at room temperature (Bowles, & Tompkins, 1989).

Fiber	E_1 (GPa)	E_2 (GPa)	G_1 (GPa)	G_2 (GPa)	ν_1	ν_2	α_1 (10^{-6}/ºC)	α_2 (10^{-6}/ºC)
T300	233.13	23.11	8.97	8.28	0.2	0.4	− 0.54	10.08
C6000	233.13	23.11	8.97	8.28	0.2	0.4	− 0.54	10.08
HMS	379.35	6.21	7.59	2.21	0.2	0.4	− 0.99	6.84
P75	550.40	9.52	6.9	3.38	0.2	0.4	− 1.35	6.84
P100	796.63	7.24	6.9	2.62	0.2	0.4	− 1.40	6.84

5.4 Boundary Conditions

There are several basic assumptions that are common to all of the methods, which are given in the previous chapter. In addition, the boundary conditions used in the finite element analyses are as follows:

- Along the planes x, y, and z = 0, the model is restricted to move in the x, y, and z directions respectively.
- The boundary planes x, y, and z = l_0 are free to move but have to remain planar in a parallel way for preserving the compatibility with adjacent cells.

5.5 Solution

The deformation in the unit cell is caused by a temperature increase of ΔT. During the deformation; x, y, and z = l_0 become, x, y, and z = l respectively and the displacement, Δl, is determined from the analysis. The CTE of the composite for the direction i is then found using

$$\alpha_i = \frac{\Delta l}{l_0}\frac{1}{\Delta T} \tag{5.1}$$

For an easier solution, edge of the representative unit cell is taken as unity and also the temperature increase is taken as unity. Then CTE of the composite for the required direction becomes the displacement of the unit cell for that direction. The displacement fields for the unit cell having a fiber volume fraction of 48% is given in Figure 5.6 and Figure 5.7.

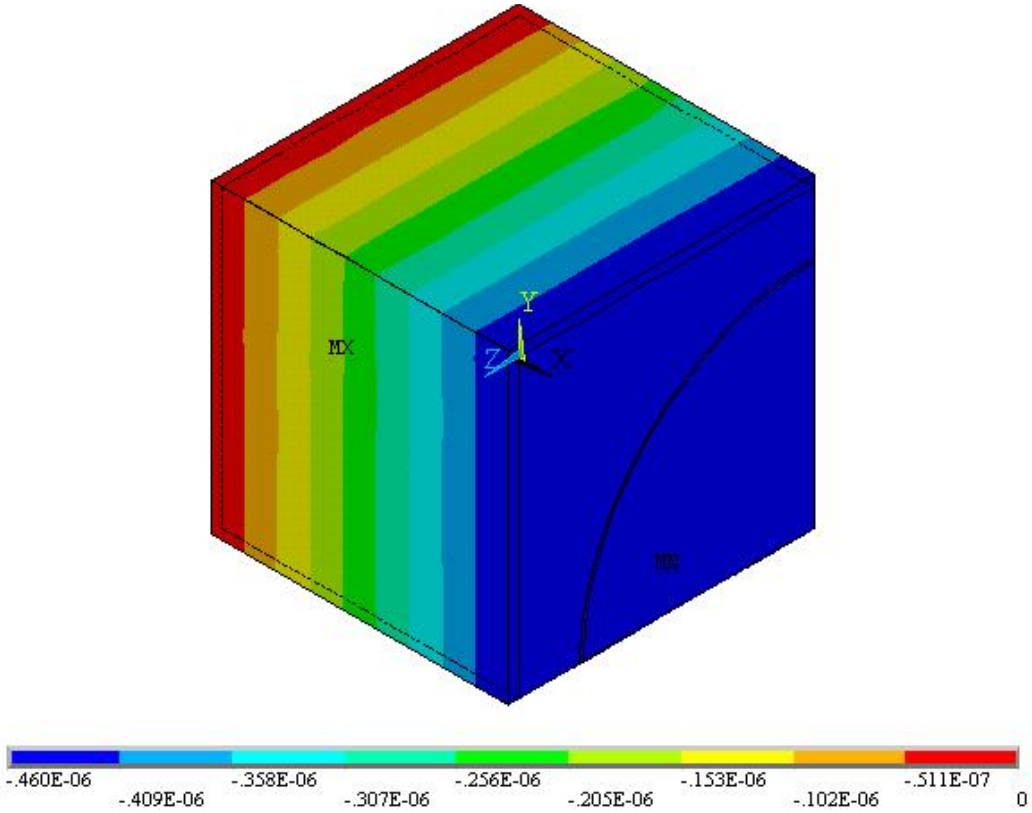


Figure 5.6 The displacement field in the longitudinal direction for the unit cell having a fiber volume fraction of 48%.

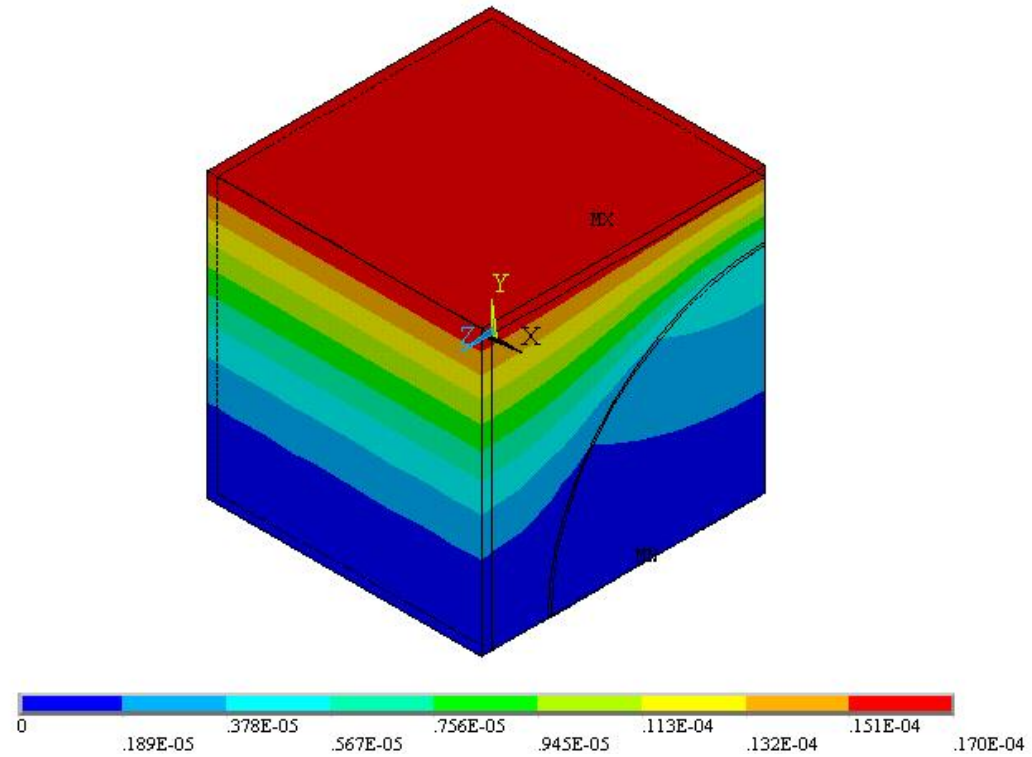


Figure 5.7 The displacement field in the transverse direction for the unit cell having a fiber volume fraction of 48%.

CHAPTER SIX
RESULTS AND DISCUSSION

Carbon fiber reinforced composite material systems had axial fiber to matrix stiffness ratios (E_{fl}/E_m) ranging from 6 to 140, and axial fiber to matrix coefficient of thermal expansion (CTE) ratios (α_{fl}/α_m) ranging from −0.01 to −0.30. Besides, glass fiber reinforced composite material had E_f/E_m of 20.6, and α_f/α_m of 10.5. Therefore, this investigation has covered a wide range of fiber/matrix combinations.

CTE predictions from some of the analytical models presented in Chapter 3 were compared with each other, with available experimental data and with finite element results for all of the material systems. Predicted and measured values for the longitudinal and transverse directions for all of the materials studied are given in Tables 6.1 and 6.2 respectively. The comparisons of these model predictions with experimental data show that for some material the agreement is very good, but for others there is some discrepancy between the experimental results and model predictions. The reason may be that the fiber-matrix interface bond which was assumed to be perfect was not really so in the experimental materials. The interface may either contain interfacial cracks or it might have elastic properties different from those of matrix and fiber.

Figures 6.1 – 6.14 show a comparison of longitudinal and transverse CTEs as a function of fiber volume fraction, predicted from the different methods for seven different material systems: E-Glass/Epoxy, T300/934 (T300/5208), P75/934 (P75/930), P75/CE339, C6000/PMR15, HMS/Borosilcate, and P100/2024Al. Experimental data are also shown on these figures.

The Shapery, Chamberlain (both hexagonal and square), Schneider, and Chamis methods all used Equation (3.14) for predicting longitudinal CTEs. As shown in the Table 6.1 and Figures 6.1, 6.3, 6.5, 6.7, 6.9, 6.11, and 6.13, the differences between the Rosen-Hashin and finite element results were negligible and there were only

small differences between these and the other results. All of the models and finite element analyses were in good agreement with the experimental data for longitudinal CTEs. The largest deviation between any of the predicted and experimental values for longitudinal CTE was 0.22 10^{-6}/°C only, in most cases the deviation was on the order of about 0.1 10^{-6}/°C, and the average deviation is 0.127 10^{-6}/°C. Although the magnitudes of longitudinal CTE differed for different material systems , the general response was the same (decreasing CTE with increasing volume fraction). This implies that the relative magnitudes of the fiber/matrix stiffness and CTE ratios did not significantly affect the general trend in longitudinal CTE as a function of volume fraction.

For the transverse CTE the Shapery results were obtained by using the modified version of the Equation (3.15) for transversely isotropic fibers, replacing fiber properties with transverse fiber properties. There were large differences between the predicted values for all of the methods, except for the Rosen-Hashin method and finite element analyses. Results from these two methods were in excellent agreement with each other. The differences between Chamis and finite element results were attributed to Poisson restraining effects which were not included in Equation (3.26). The omission of this type of three dimensional effects was also thought to be responsible for the large difference between the Chamberlain, Schneider, and finite element results. These differences have been previously documented in the literature (Bowles, & Tompkins, 1989).

Results also show that the Rosen-Hashin and finite element results for transverse CTE were generally in much better agreement with the experimental data, than the other methods for all materials investigated. The Shapery results were in good agreement with experimental results and were in better agreement with the experimental data for the P75/930 and P75/CE339 material systems. However, it should be noted that the matrix mechanical properties for these two systems were assumed to be the same as the other epoxy matrices, which is probably not an accurate assumption, and therefore the better agreement with the experimental data is believed to be coincidental. It should also be remembered that the modification of the

Shapery's method for transversely isotropic fibers was not based on any mathematical derivation, and was included for comparison purposes only. Agreement between experimental values and Rosen-Hashin and finite element predicted values were usually within about 15%. Predictions from the other methods differed with the experimental data by as much as 50%. The largest deviation between any of the predicted and experimental values for transverse CTE was 27.09 10^{-6}/°C, in most cases the deviation was on the order of about 10 10^{-6}/°C, and the average deviation is 6.45 10^{-6}/°C.

Unlike the results for longitudinal CTE, the response of transverse CTE as a function of volume fraction was affected by the fiber/matrix property ratios. E-Glass/ Epoxy, T300/934 and P75/934, P75/CE339 and C6000/PMR15 had similar fiber/matrix property ratios, and exhibited a similar response (Figures 6.2, 6.4, 6.6, 6.8, and 6.10). Decreasing fiber/matrix moduli ratio approximates the finite element results to other analytical methods, except for the Shapery results. The P100/2024Al system (Figure 6.14) had CTE ratios similar to T300/934 and P75/934, but had much smaller moduli ratios. This difference in moduli ratios resulted in a different response of transverse CTE as a function of volume fraction as predicted from the finite element analyses; increasing transverse CTE with increasing volume fraction upto 30% of fiber volume fraction. The HMS/Borosilicate glass (BG) system (Figure 6.12) had much larger CTE property ratios from other material systems. The ratio of longitudinal to transverse CTEs was 2.1 for the HMS/Borosilicate system compared to values ranging from 0.1 to 0.3 for the other material systems evaluated. This difference caused a significantly different response in transverse CTE as a function of volume fraction, increasing transverse CTE with increasing volume fraction for all values of volume fraction.

Table 6.1 Comparison of the experimental results for longitudinal CTEs of different composite materials with calculated values using different analytical models, and finite element method.

Material (Fiber/Matrix)	Fiber volume fraction (%)	Shapery, Van Fo Fy (10^{-6}/ºC)	Chamberlain (Hexagonal) (10^{-6}/ºC)	Chamberlain (Square) (10^{-6}/ºC)	Rosen-Hashin* (10^{-6}/ºC)	Schneider (10^{-6}/ºC)	Chamis (10^{-6}/ºC)	ANSYS (10^{-6}/ºC)	Experimental* (10^{-6}/ºC)
E-glass/ Epoxy	60	6.49	6.49	6.49	-	6.49	6.49	6.78	6.57
T300/5208	68	-0.153	-0.153	-0.153	-0.091	-0.153	-0.153	-0.070	-0.113
T300/934	57	0.077	0.077	0.077	0.160	0.077	0.077	0.170	-0.002
P75/934	48	-0.966	-0.966	-0.966	-0.921	-0.966	-0.966	-0.921	-1.051
P75/930	65	-1.158	-1.158	-1.158	-1.128	-1.158	-1.158	-1.125	-1.076
P75/CE339	54	-0.917	-0.917	-0.917	-0.858	-0.917	-0.917	-0.857	-1.020
C6000/PMR15	63	-0.225	-0.225	-0.225	-0.187	-0.225	-0.225	-0.178	-0.212
HMS/Borosilicate	47	-0.325	-0.325	-0.325	-0.324	-0.325	-0.325	-0.325	-0.414
P100/2024 Al	40	1.579	1.579	1.579	1.632	1.579	1.579	1.638	1.440

* Bowles and Tompkins (1989)

Table 6.2 Comparison of the experimental results for transverse CTEs of different composite materials with calculated values using different analytical models, and finite element method.

Material (Fiber/Matrix)	Fiber volume fraction (%)	Shapery, Van Fo Fy (10^{-6}/ºC)	Chamberlain (Hexagonal) (10^{-6}/ºC)	Chamberlain (Square) (10^{-6}/ºC)	Rosen-Hashin* (10^{-6}/ºC)	Schneider (10^{-6}/ºC)	Chamis (10^{-6}/ºC)	ANSYS (10^{-6}/ºC)	Experimental* (10^{-6}/ºC)
E-glass/ Epoxy	60	30.26	17.44	13.39	-	22.79	19.95	25.83	30
T300/5208	68	28.91	16.53	13.44	24.48	19.11	18.84	23.86	25.54
T300/934	57	33.89	19.97	17.13	29.70	23.69	22.3	29.45	29.03
P75/934	48	36.26	20.97	18.13	34.02	23.94	23.18	34.04	34.52
P75/930	65	27.74	14.85	11.52	25.02	16.94	17.16	24.96	31.72
P75/CE339	54	45.46	24.93	20.32	42.66	29.1	28.0	42.70	47.41
C6000/PMR15	63	26.96	16.11	13.84	22.32	18.41	18.15	22.18	22.43
HMS/Borosilicate	47	6.657	5.487	5.737	4.48	5.899	6.026	4.49	3.78
P100/2024 Al	40	21.8	14.49	13.4	27	12.44	15.64	26.96	26.12

* Bowles and Tompkins (1989)

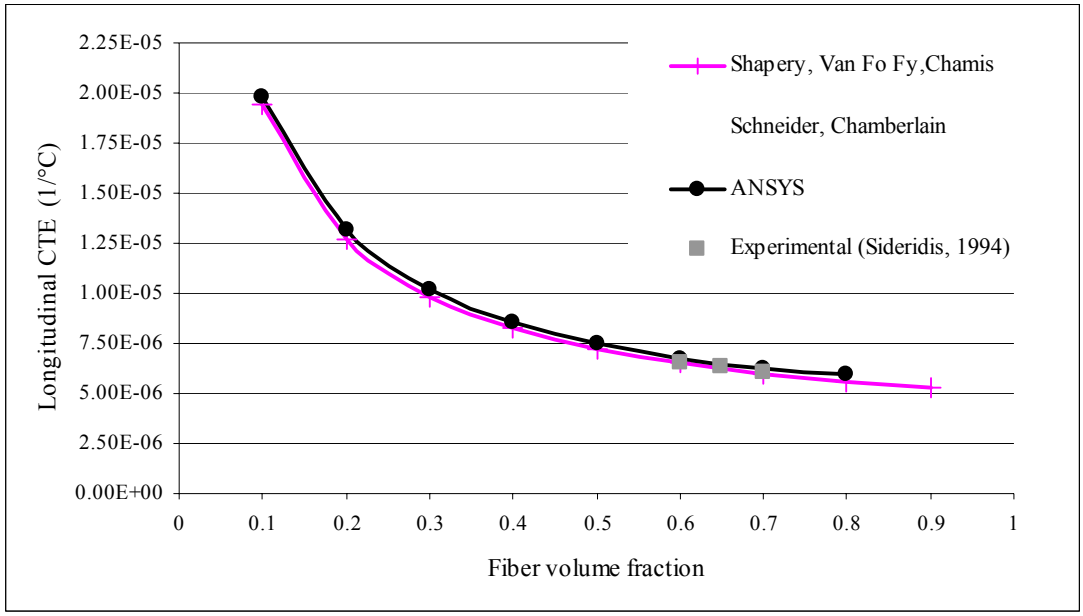


Figure 6.1 Longitudinal CTE of E-Glass/Epoxy composite.

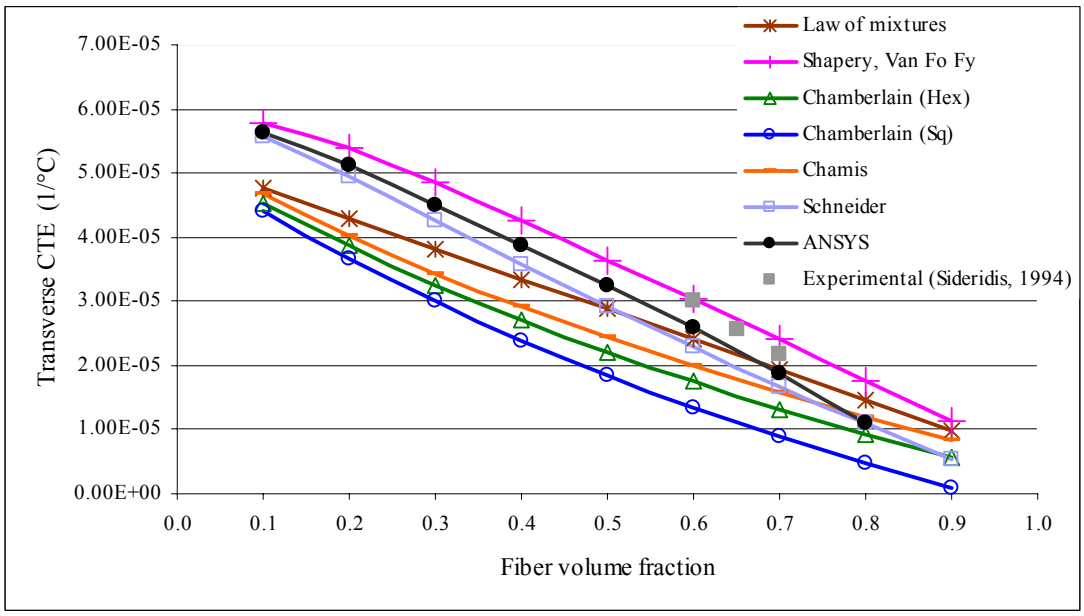


Figure 6.2 Transverse CTE of E-Glass/Epoxy composite.

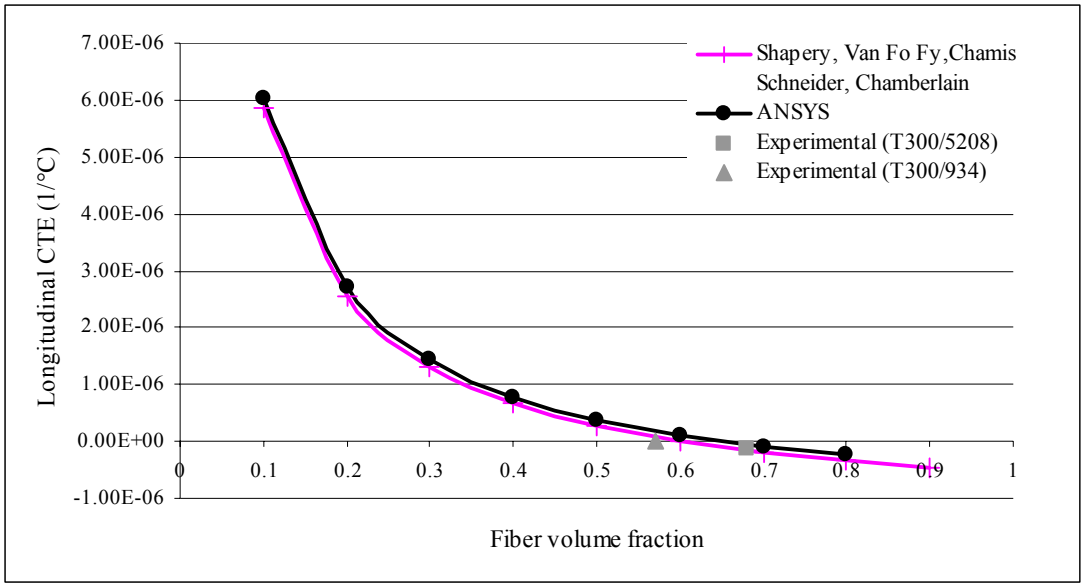


Figure 6.3 Longitudinal CTE of T300/5208, and T300/934 composites.

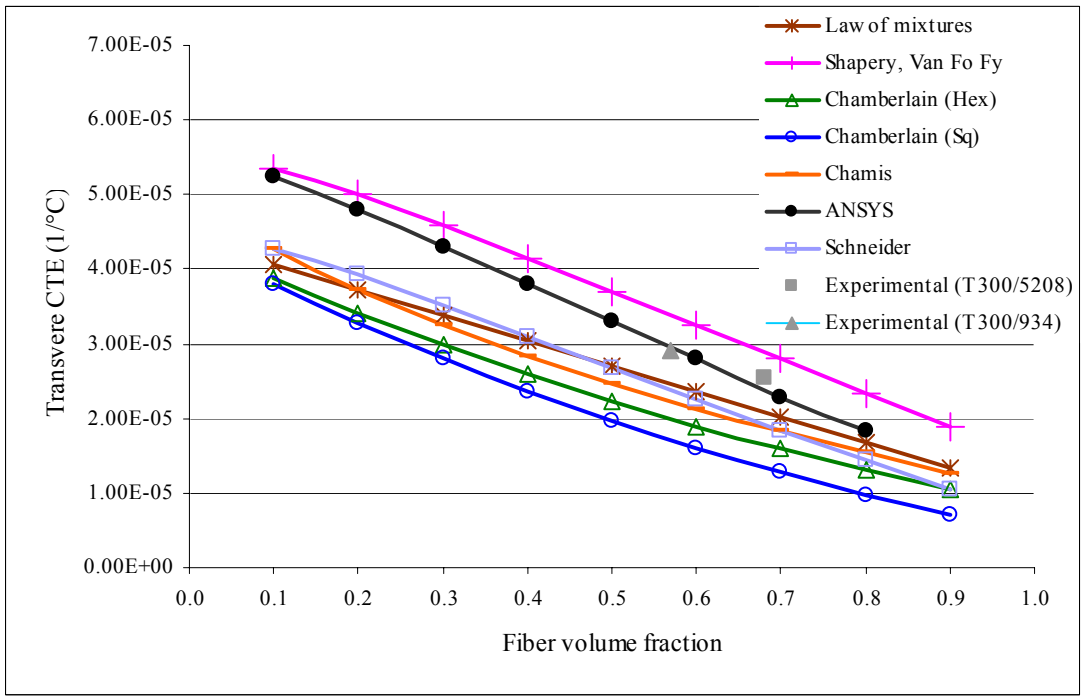


Figure 6.4 Transverse CTE of T300/5208, and T300/934 composites.

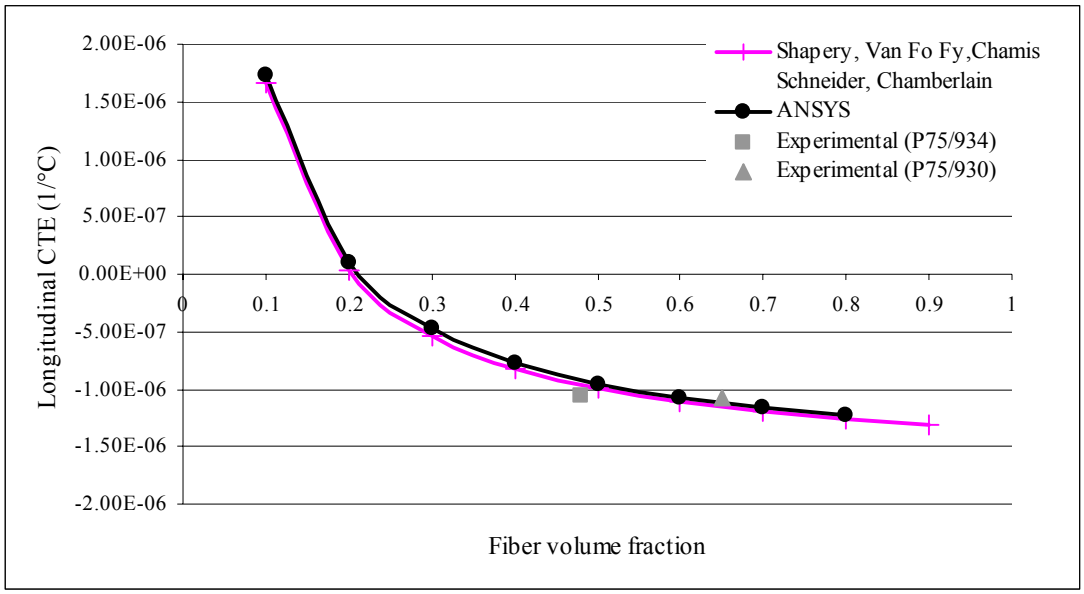


Figure 6.5 Longitudinal CTE of P75/934, and P75/930 composites.

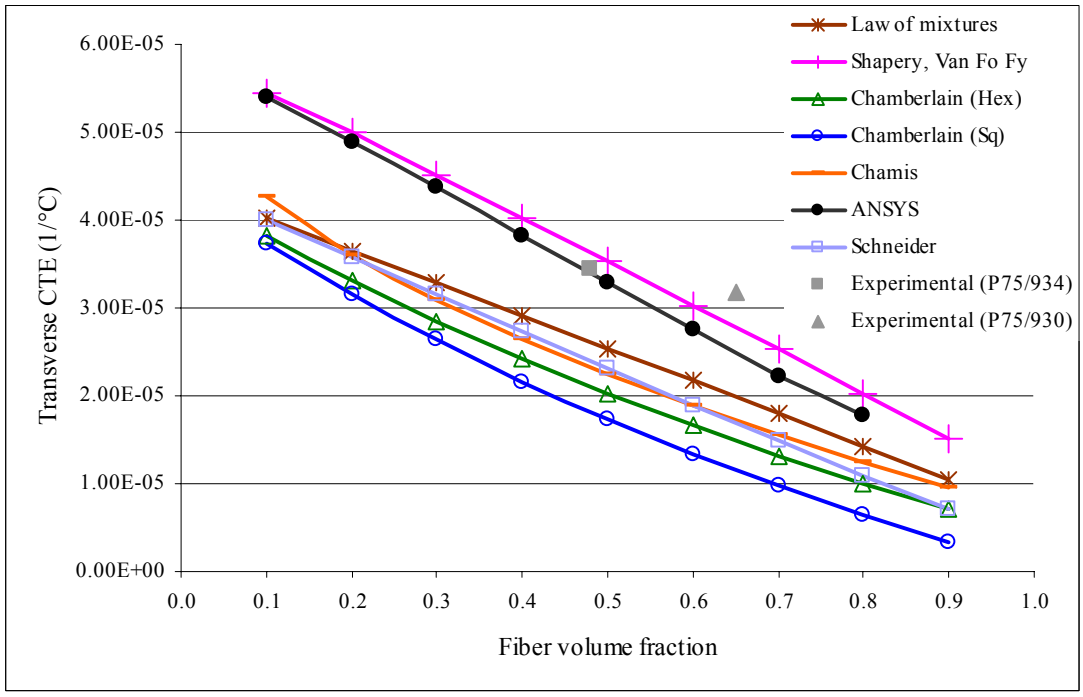


Figure 6.6 Transverse CTE of P75/934, and P75/930 composites.

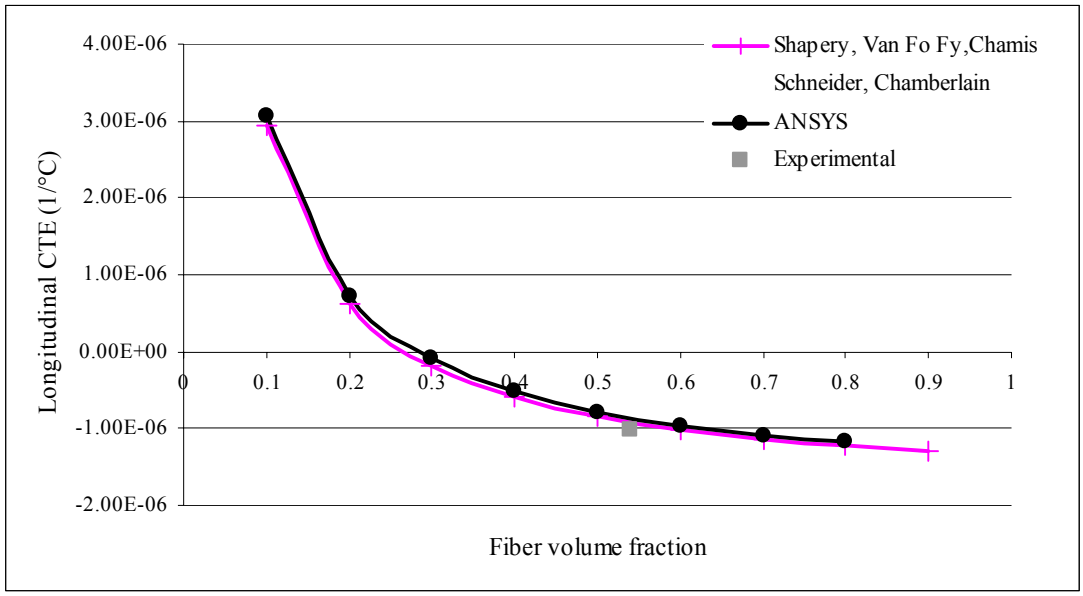


Figure 6.7 Longitudinal CTE of P75/CE339 composite.

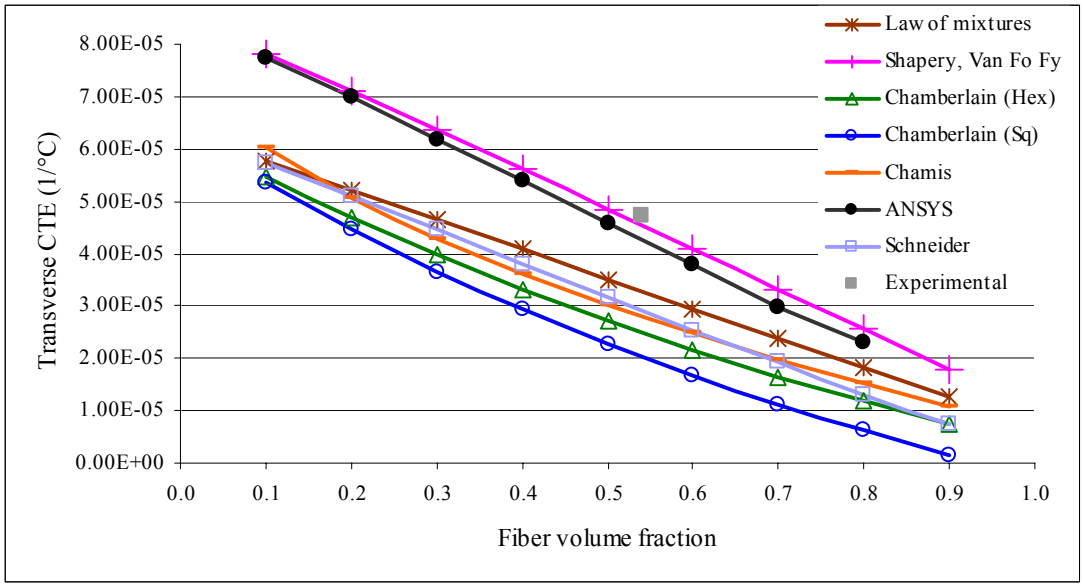


Figure 6.8 Transverse CTE of P75/CE339 composite.

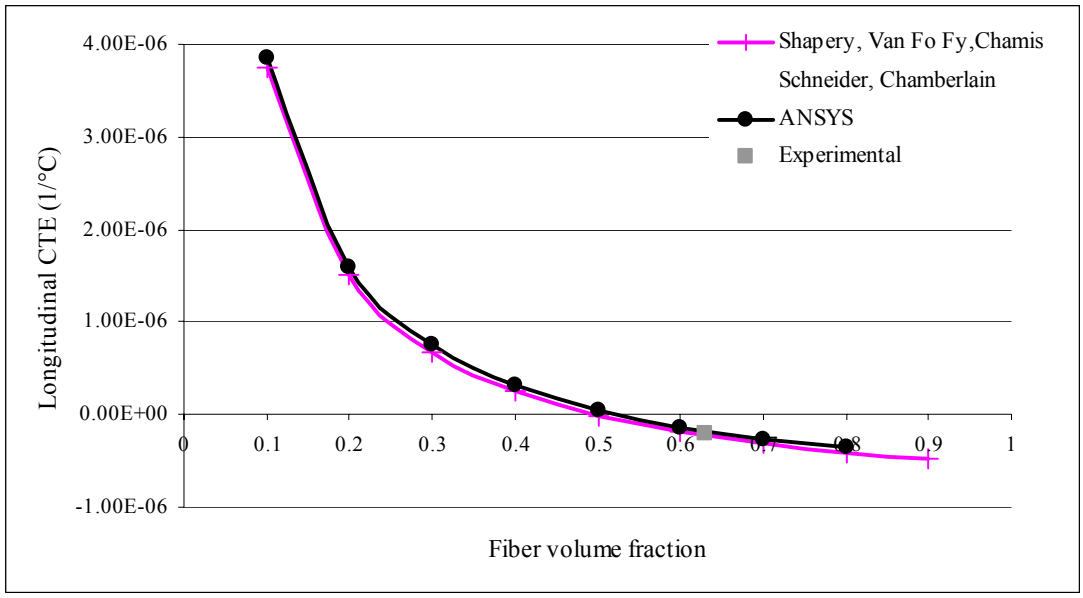


Figure 6.9 Longitudinal CTE of C6000/PMR15 composite.

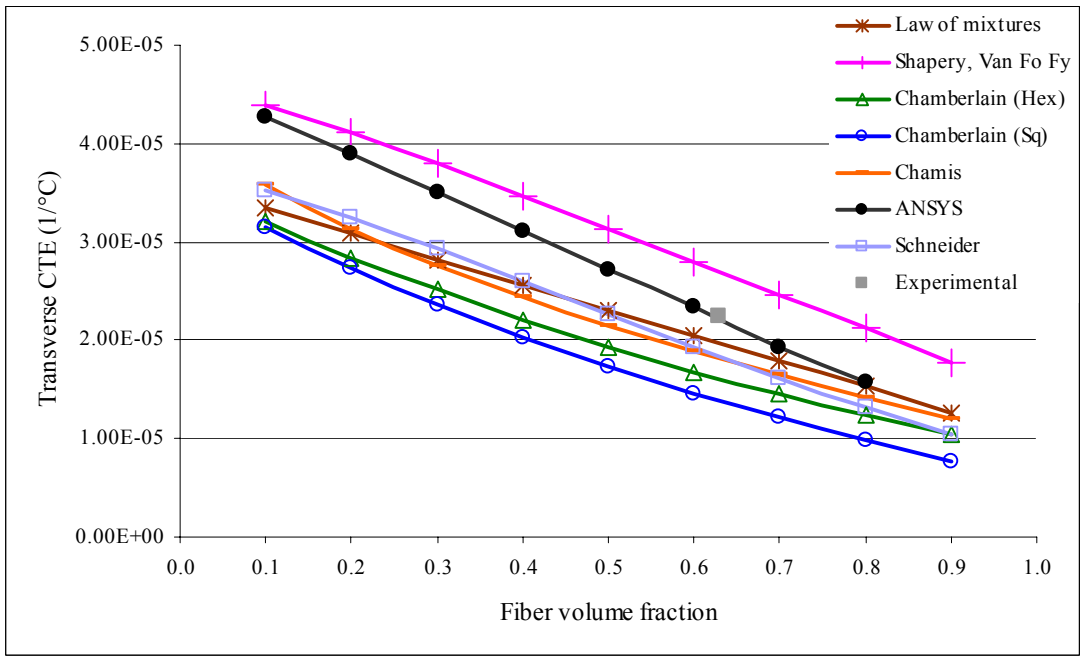


Figure 6.10 Transverse CTE of C6000/PMR15 composite.

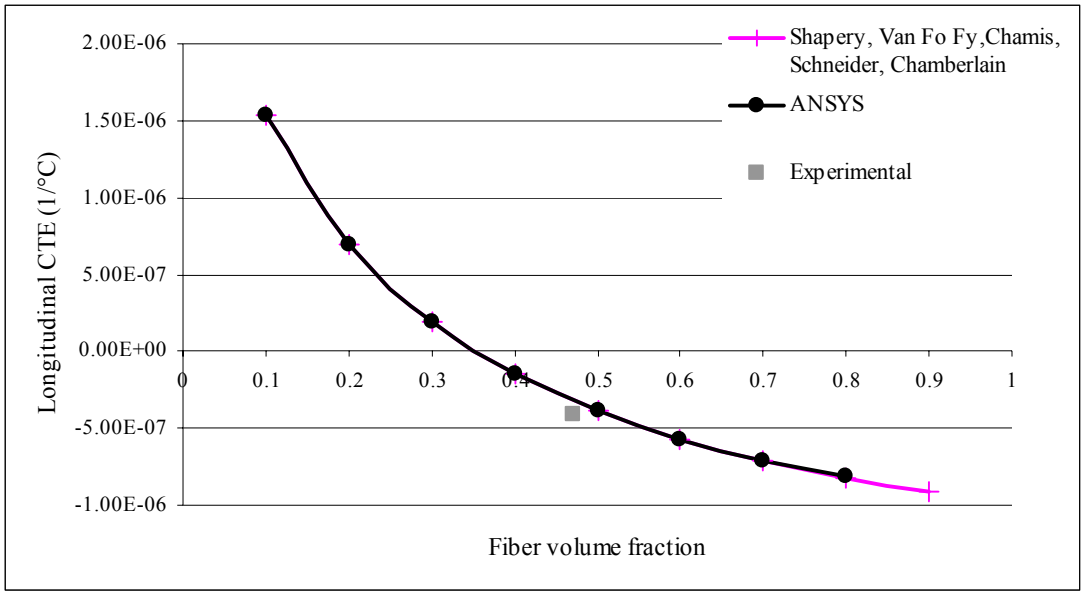


Figure 6.11 Longitudinal CTE of HMS/BG composite.

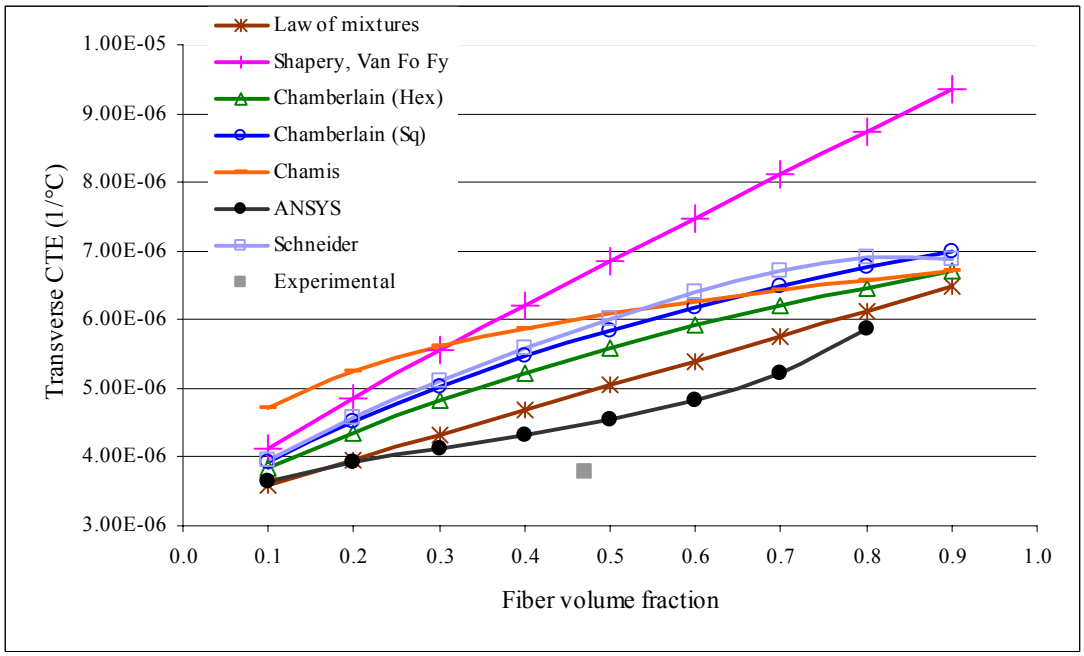


Figure 6.12 Transverse CTE of HMS/BG composite.

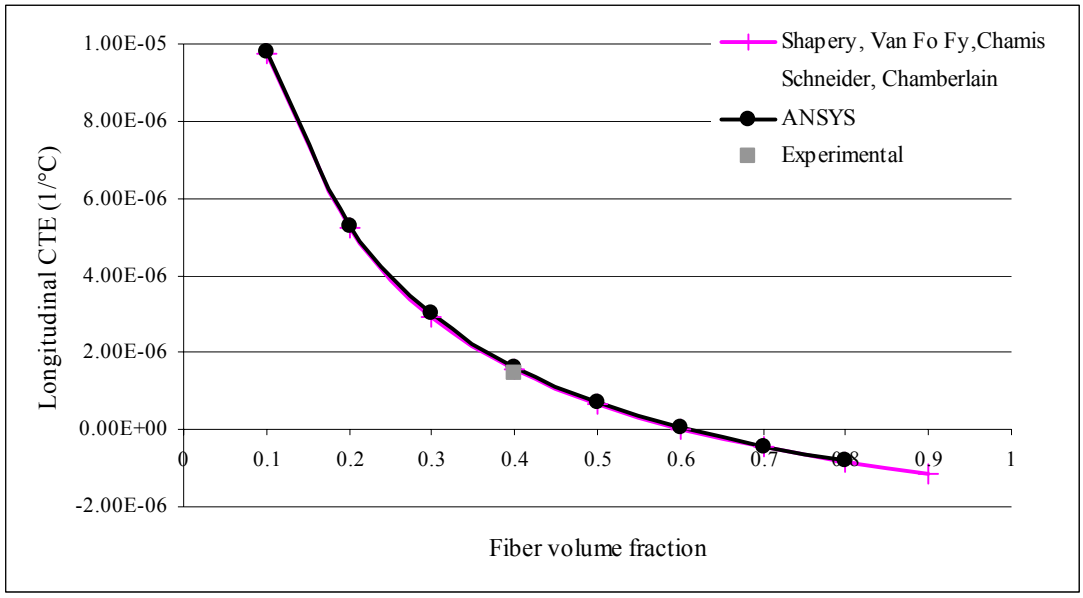


Figure 6.13 Longitudinal CTE of P100/2024Al composite.

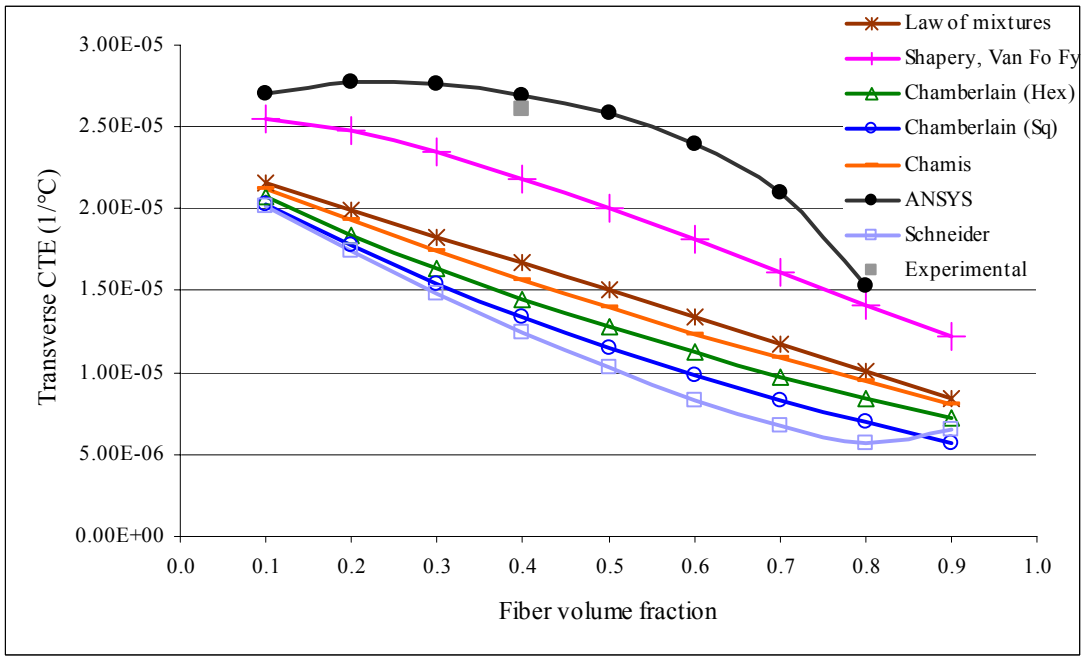


Figure 6.14 Transverse CTE of P100/2024Al composite.

REFERENCES

Adams, D.F., & Crane D.A. (1984). Combined loading micromechanical analysis of a unidirectional composite. *Composites, 15 (3)*, 181-192.

Bowles, D.E., & Tompkins S.S. (1989). Prediction of coefficients of thermal expansion for unidirectional composites. *Journal of Composite Materials, 23*, 370-388.

Callister, W.D. (1994). *Materials science and engineering; an introduction* (3rd ed.). New York: John Wiley & Sons, Inc.

Chamis, C.C., & Sendecky G.P. (1968). Critique on theories predicting thermoelastic properties of fibrous composites. *Journal of Composite Materials, 2 (3)*, 332-358.

Chandrupatla, T.R., & Belegundu A.D. (2002). *Introduction to Finite Elements in Engineering* (3rd ed.). New Jersey: Prentice Hall.

Chawla, K.K. (1998). *Composite materials science and engineering* (2nd ed.). New York: Springer-Verlag.

Foye, R.L. (1968). Advanced design concepts for advanced composite airframes. *Technical Report AFML-TR-68-91*. Columbus: North American-Rockwell Corporation.

Hashin, Z. (1979). Analysis of properties of fiber composites with anisotropic constituents. *Journal of Applied Mechanics, 46*, 543-550.

Hill, R. (1964). Theory of mechanical properties of fibre-strengthened materials: 1. elastic behavior. *Journal of the Mechanics and Physics of Solids, 12 (4)*, 199-212.

IARC, 1988. Man-made Fibers and Radon. *IARC Monographs on the Evaluation of Carcinogenic Risk of Chemicals to Humans, 43*. 300.

Ishikava, T., Koyama, K., & Kobayashi, S. (1978). Thermal expansion coefficients of unidirectional composites. *Journal of Composite Materials, 12*, 153-168.

Islam, MD.R., Sjölind, S.G., & Pramila A. (2001). Finite element analysis of linear thermal expansion coefficients of unidirectional cracked composites. *Journal of Composite Materials, 35*, 1762-1776.

Johnson, R.R., Kural M.H., & Mackey G.B. (1981) *Thermal expansion properties of composite materials*. California: Lockheed Missiles and Space Co. Inc.

Jones, R.M. (1999). Mechanics of composite materials (2nd ed.). Philadelphia: Taylor and Francis.

Levin, V.M. (1967). On the coefficients of thermal expansion of heterogeneous materials (in Russian). *Mekhanika Tverdogo Tela*, 88.

Moaveni, S. (1999). *Finite element analysis theory and application with ANSYS*. New Jersey: Prentice Hall.

Morrell, R. (1997). Thermal property measurement and data on composite materials. *Measurement Note CMMT(MN)011*. London: National Physical Laboratory.

Rogers, K.F., Phillips, L.N., Kingston-Lee, D.M., Yates, B., Overy M.J., Sargent, J.P., et al. (1977).The thermal expansion of carbon fibre-reinforced plastics. *Journal of Materials Science, 12*, 718-734.

Rosen, B.W. & Hashin, Z. (1970). Effective thermal expansion coefficients and specific heats of composite materials. *International Journal of Engineering Science, 8*, 157-173.

Rupnowski, P., Gentza, M., Sutterb, J.K., & Kumosa M. (2005). An evaluation on the elastic properties and thermal expansion coefficients of medium and high modulus graphite fibers. *Composites: Part A, 36* (3), 327-338

Schapery, R.A. (1968). Thermal expansion coefficients of composite materials based on energy principles. *Journal of Composite Materials, 2 (3)*, 380-404.

Shen, Y.L. (1998). Thermal Expansion of Metal-Ceramic Composites: A Three Dimensional Analysis. *Materials Science and Engineering A, 252*, 269-275.

Sideridis, E. (1994). Thermal expansion coefficient of fiber composites defined by the concept of the interphase. *Composites Science and Technology, 51*, 301-317.

Technical note 69: Principles of Push-Rod Dilatometry, (n.d.). Retrieved July 11, 2005 from http://www.anter.com/TN69.htm

Thermal expansion (n.d) Retrieved July 11, 2005 from http://www.pmiclab.com/testing/ThermalExpansion.html

Tantina, G., Nimmer, R., (1994). *Structural analysis of thermoplastic components.* Malnati P. (Ed.). New York: McGraw-Hill, Inc.

Tsai, S.W., & Hahn, H. T. (1980). *Introduction to composite materials*. Lancester: Technomic Publishing Co. Inc.

Wypych G. (2000). *Handbook of fillers* (2nd ed.). Toronto: ChemTec Publishing.

Van Fo Fy, G. A. (1965). Thermal strains and stresses in glass fiber reinforced media (in Russian). *Prikl. Mekh. Teor. Fiz.*, 101.

Van Fo Fy, G. A., & Savin G. N. (1965). Fundamentals of the theory of non-fabric glass reinforced plastics (in Russian). *Mekhanika Polimerov, 1*, 151.

Van Fo Fy, G. A. (1966). Elastic constants and thermal expansion of certain bodies with inhomogeneous regular structure (in Russian). *Soviet Physics, Doklady, 11*, 176.

Van Fo Fy, G. A. (1966). Basic relations of the theory of oriented glass reinforced plastics with hollow fibers (in Russian). *Mekhanika Polimerov, 2*, 763.